

AD-A055 073

AIR FORCE INST OF TECH WRIGHT-PATTERSON AFB OHIO  
AN ANALYSIS OF METALLIC GLASSES BY MOSSBAUER SPECTROSCOPY.(U)  
MAR 78 T A SCHMIDT  
GNE/PH/78M-8

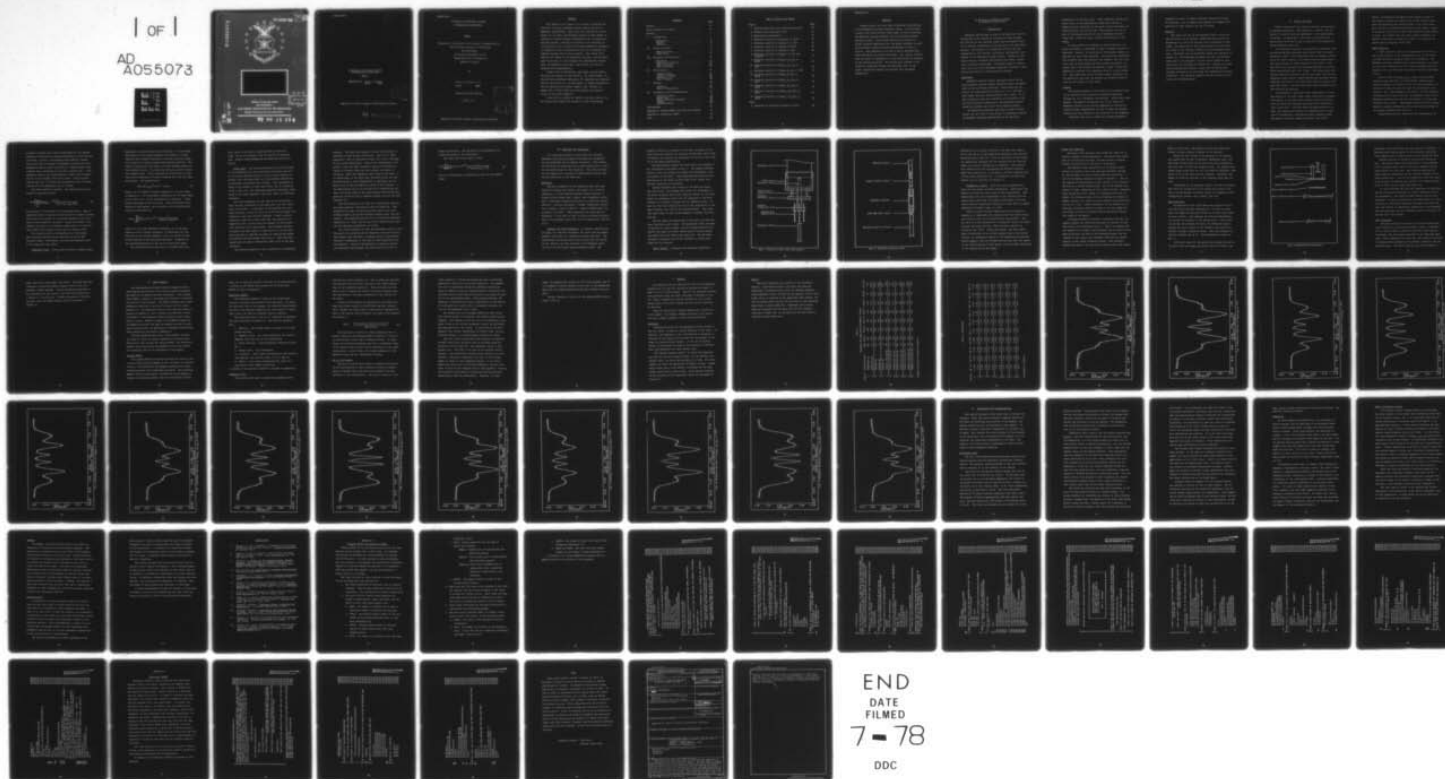
F/G 11/6

UNCLASSIFIED

NL

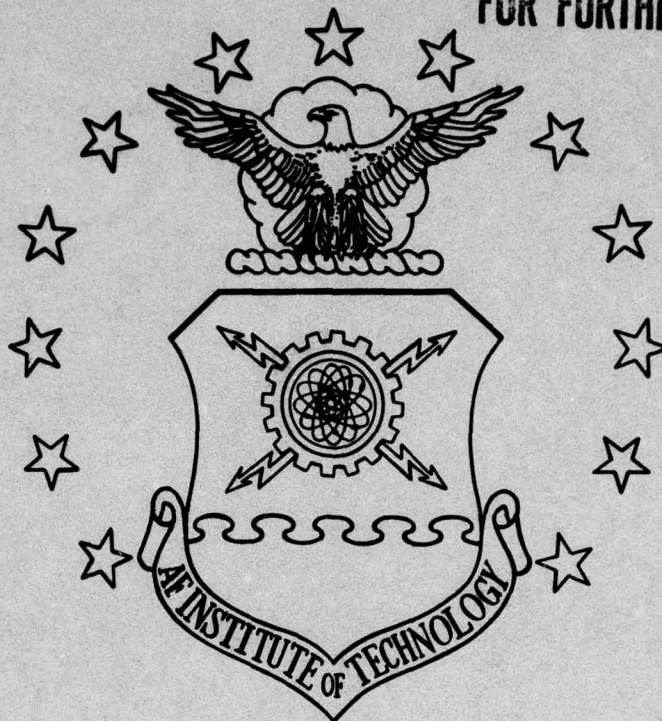
1 OF 1

AD  
A055073



AD A 055073

FOR FURTHER TRAN



(1)

See 1473  
in back



UNITED STATES AIR FORCE  
AIR UNIVERSITY

AIR FORCE INSTITUTE OF TECHNOLOGY

Wright-Patterson Air Force Base, Ohio

DDC  
RECEIVED  
JUN 15 1978  
A

AD No. \_\_\_\_\_  
DDC FILE COPY

78 06 15 074

GNE/PH/78M-8

1

AN ANALYSIS OF METALLIC GLASSES  
BY MOSSBAUER SPECTROSCOPY

THESIS

GNE/PH/78M-8    Terry A. Schmidt  
Major                      USAF

DDC  
RECEIVED  
JUN 15 1978  
A

Approved for public release; distribution unlimited

78 06 15 074

GNE/PH/78M-8

AN ANALYSIS OF METALLIC GLASSES  
BY MOSSBAUER SPECTROSCOPY

THESIS

Presented to the Faculty of the School of Engineering of  
The Air Force Institute of Technology  
Air University  
in Partial Fulfillment of the  
Requirements for the Degree of  
Master of Science

by

Terry A. Schmidt, B. S.

Major

USAF

Graduate Nuclear Effects

March 1978

ACCESSION NO.	
NTIS	Write Section <input checked="" type="checkbox"/>
DOC	Get Section <input type="checkbox"/>
UNCLASSIFIED	<input type="checkbox"/>
CLASSIFICATION	
BY	
DISTRIBUTION/AVAILABILITY CODES	
Dist.	AVAIL. CODE OR SPECIAL
A	

Approved for public release; distribution unlimited.

412244

hc



## Preface

This thesis is the result of my efforts to analyze the structure of several amorphous alloys through the use of Mossbauer spectroscopy. There were four objectives in this study: (1) to obtain the Mossbauer spectra of each sample at room and at liquid nitrogen temperatures; (2) to analyze the obtained spectra, relating the results to the structure of the materials; (3) to modify the existing Mossbauer equipment to simplify the use and adjustment; and (4) to simplify the computer program used in data analysis. This thesis will describe the theory of the amorphous structure, and the model used to describe it, the equipment and experimental methods used, the analysis of the data, the results, and the conclusions and recommendations.

I would like to acknowledge, and thank, several people who were most helpful in this project. Dr. Harold Gegel, of the Air Force Materials Laboratory, for supplying the materials used in this study; Dr. Jon Spijkerman, of Ranger Electronics, for his material and personal support; and, finally, Dr. George John, without whose help and guidance this project could not have been completed.

I also wish to express my thanks to my wife, Denise, for her unwaivering support and patience in this undertaking.

## Contents

	Page
Preface . . . . .	ii
List of Figures and Tables . . . . .	iv
Abstract . . . . .	v
I. Introduction . . . . .	1
Background . . . . .	1
Purpose . . . . .	2
Overview . . . . .	3
II. Theory and Model . . . . .	4
Model Selection . . . . .	5
Final Model . . . . .	8
III. Equipment and Procedures . . . . .	11
Equipment . . . . .	11
Source and Absorbers . . . . .	16
Data Collection . . . . .	17
Data Processing . . . . .	19
IV. Data Analysis . . . . .	21
Program GENFIT . . . . .	21
Subroutine CALFUN . . . . .	22
Goodness of Fit . . . . .	22
Use of Program . . . . .	23
V. Results . . . . .	26
Certainty . . . . .	26
Table I (Discussion) . . . . .	27
VI. Conclusions and Recommendations . . . . .	43
Structural Model . . . . .	43
Exceptions . . . . .	46
Model Independent Results . . . . .	47
Summary . . . . .	48
Recommendations . . . . .	48
Bibliography . . . . .	50
Appendix A: Program GENFIT and Subroutine READIN . . . . .	51
Appendix B: Subroutine CALFUN . . . . .	63
Vita . . . . .	67

## List of Figures and Tables

Figure	Page
1 Modified Mossbauer Drive and Extension Mount	13
2 Modified Drive Extension Shaft . . . . .	14
3 Experimental Arrangement . . . . .	18
4 Mossbauer Spectrum of Fe <sub>80</sub> P <sub>13</sub> C <sub>7</sub> at 300°K . .	30
5 Mossbauer Spectrum of Fe <sub>80</sub> P <sub>13</sub> C <sub>7</sub> at 75°K . .	31
6 Mossbauer Spectrum of Fe <sub>80</sub> B <sub>20</sub> at 300°K . . .	32
7 Mossbauer Spectrum of Fe <sub>80</sub> B <sub>20</sub> at 75°K . . .	33
8 Mossbauer Spectrum of Fe <sub>80</sub> B <sub>20</sub> at 75°K and Degaussed . . . . .	34
9 Mossbauer Spectrum of Fe <sub>80</sub> P <sub>11.7</sub> C <sub>6.3</sub> B <sub>2</sub> at 300°K . . . . .	35
10 Mossbauer Spectrum of Fe <sub>80</sub> P <sub>11.7</sub> C <sub>6.3</sub> B <sub>2</sub> at 75°K . . . . .	36
11 Mossbauer Spectrum of Fe <sub>80</sub> P <sub>8.5</sub> C <sub>4.5</sub> B <sub>7</sub> at 75°K	37
12 Mossbauer Spectrum of Fe <sub>80</sub> P <sub>8.5</sub> C <sub>4.5</sub> B <sub>7</sub> at 300°K . . . . .	38
13 Mossbauer Spectrum of Fe <sub>80</sub> P <sub>6.5</sub> C <sub>3.5</sub> B <sub>10</sub> at 75°K . . . . .	39
14 Mossbauer Spectrum of Fe <sub>80</sub> P <sub>6.5</sub> C <sub>3.5</sub> B <sub>10</sub> at 300°K . . . . .	40
15 Mossbauer Spectrum of Fe <sub>80</sub> P <sub>11.6</sub> C <sub>6.3</sub> Si <sub>2</sub> at 75°K . . . . .	41
16 Mossbauer Spectrum of Fe <sub>80</sub> P <sub>11.7</sub> C <sub>6.3</sub> Si <sub>2</sub> at 300°K . . . . .	42
 Table	
I Measured and Calculated Parameter Values . .	28

Abstract

Several models have been used to describe the structure of iron-phosphorous-carbon amorphous alloys. In this study a twelve site substitutional solid model is used to describe the Mossbauer spectra obtained from six different metallic amorphous alloys. Spectra were obtained at room and at liquid nitrogen temperatures for the parent material, as well as for alloys containing various percentages of boron or silicon. Each spectrum is fit with a sum of Lorentzian profiles describing the twelve site model. The results indicate that the model is inadequate in fully describing the structure of the various materials. The results also indicate a difference in structure between the materials, and, in two cases, significant changes in structure with decreased temperature.



# AN ANALYSIS OF METALLIC GLASSES BY MOSSBAUER SPECTROSCOPY

## I. Introduction

Mossbauer spectroscopy is used as an analytical tool in disciplines as far ranging as biology and lunar seology. The wide use of the technique stems from the method's ability to provide information on the environs of an individual nucleus. The analysis of a Mossbauer spectrum can give information on the chemical, electrical, and magnetic environment of the Mossbauer-isotope nucleus. Because of this unique ability, Mossbauer spectroscopy has become a major tool in physical metallurgy. The analyst hopes to extrapolate from the various Mossbauer parameters obtained, information descriptive of the macroscopic material.

### Background

Amorphous metallic alloys, sometimes called the metallic glasses, exhibit several properties which recommend their use as structural materials. Among these are flexibility and high strength (as high as  $2$  to  $4 \times 10^5$  psi) -- both highly desirable characteristics (Ref 1:563). It is these properties that have attracted the attention of the Air Force Materials Laboratory to the amorphous metallic alloys for possible use in Air Force weapons systems.

The Materials Laboratory has begun a study of these alloys, and as a part of that study, is examining a series of amorphous compounds manufactured by the Battelle

Laboratories at Columbus, Ohio. These materials consist of a parent alloy of iron-phosphorous-carbon and a series of daughter alloys consisting of the parent alloy with added, or substitutional, boron or silicon. The presence of iron in each of the samples permits the use of Mossbauer spectroscopy with a cobalt-57 source without modification to the sample.

To fully predict the response of these materials to a given environment, a knowledge of their internal structure is desirable. However, the structure of the metallic glassy alloys has not been fully described. Various models describing the structure have been proposed (for example, Ref 2,3); however, none of these models has been totally successful, although each of the models does provide a means to describe a property or reaction of an amorphous alloy to a given stimulus. This study uses one of the many models, primarily for its simplicity, and does not address its validity except in terms of the results of this study.

#### Purpose

The primary purpose of this study was to determine what can be learned of the structure of amorphous materials through the use of Mossbauer spectroscopy. Within this broad purpose, the specific objectives were (1) to obtain the Mossbauer spectra of the various compounds at room and at liquid nitrogen temperatures, and (2) to begin an analysis relating the data obtained to the structure of the compound.

Secondary aims were to modify the existing Mossbauer

equipment in order to improve spectrum resolution and ease of adjustment, and to simplify and upgrade the computer program used in data analysis and curve fitting.

### Overview

The theory and use of the Mossbauer effect using a cobalt-57 source and an absorber containing iron-57 are well documented (e.g. Ref 4,5) and will not be discussed in this study. The completion of this study required the selection of a model of the internal structure of the amorphous materials. That model and the associated theory are discussed in Chapter II. The Mossbauer equipment used and the modifications made to the equipment, as well as the method of data collection, are discussed in Chapter III. Chapter IV covers data processing and analysis, along with the significant problems encountered in describing the experimentally-obtained spectra. The remaining chapters discuss results, conclusions, and recommendations.

## II. Theory and Model

Various models have been used to describe the structure of amorphous materials. This discussion, however, will be limited to several which are applicable to the glassy metallic alloys. In particular, this study is concerned with those models which can be used to describe iron-phosphorous-carbon amorphous materials.

In an amorphous material, the atoms have coagulated into an extraordinarily disordered state rather than the normal crystalline state. This disordered state is normally achieved by the rapid cooling of the molten state by splat quenching, spin cooling, or vapor deposition (Ref 6:231). Polk and others have described the resulting material as a solidified supercooled liquid (Ref 7:486). The diffuse halo diffraction patterns obtained by Fujita and others from various amorphous alloys exhibit random distribution patterns clearly different from that of the liquid from which the alloys were made (Ref 6:231). In both cases their results implied a random distribution function.

Polk proposed a structural model consisting of "a random packing of the metal atoms, which would have an arrangement similar to the hard sphere packing studied by Bernal, with the metalloid occupying the larger holes inherent in such a structure." The hard sphere packing referred to by Polk, and described by Bernal, has idealized holes in the form of tetrahedrons, octahedrons, capped trigonal prisms, and several even more complex geometries (Ref 7:487).



Fujita, in studying an amorphous alloy similar to that of this report, modeled the structure as a body centered cubic with the metalloid atoms substitutional in the cubic structure, as well as existing interstitially (Ref 6:232). Tsuei, in an earlier work done in 1968, also assumed the body centered cubic, but treated only the eight nearest neighbors, as opposed to Fujita's treatment of a total of 14 nearest and second nearest neighbors (Ref 8:605).

#### Model Selection

A basic question, then, in the selection of a model to use in the analysis of the experimental data, is the number of first and second neighbor atoms to be considered. The Mossbauer spectrum obtained from a given material is a result of the total interaction of all of these neighbors with the absorber atom; and the model must account for each individual effect.

Tsuei's study of  $\text{Fe}_{80}\text{P}_{12.5}\text{C}_{7.5}$  (where the subscripts indicate atomic percent), as noted before, assumed eight nearest neighbors, but used only the five most prominent combinations of iron and non-iron atoms in his computer curve fitting. Here, and throughout this study, the most prominent combinations are those which have the greatest effect on the Mossbauer absorber atom and will be referred to as the most prominent iron "sites". The results obtained by Tsuei approximated a binomial distribution of iron and non-iron atoms in the nearest neighbor shell (Ref 8).

Complicating Tsuei's results was the determination by

Lin that a similar alloy could be described by 13.6 nearest neighbors consisting of a random distribution of iron and non-iron atoms. Fujita, in discussing these results, reports that he was able to analyze the Mossbauer patterns for iron-phosphorous-carbon alloys by assuming a "nearly perfect body centered cubic consisting of very small crystallites." This assumption lead to the consideration of eight first neighbor and six second neighbor sites (Ref 6:232). While Fujita's results work well in fitting the experimental data, two problems exist in the application of his scheme.

The first problem is expense. The equation used to describe the spectrum becomes

$$I(x) = \sum_{i=0}^6 \sum_{n=0}^8 \sum_{m=0}^6 \frac{\pi A_{in}}{\Gamma} \frac{C C_c (1-c)^{14-n-m}}{8^{n6m}} \frac{1}{1 + [(x - x_i - \delta_{\alpha_i n} - \delta_{\beta_i m}) / \Gamma]^2} \quad (1)$$

The meaning of these terms will be discussed later. What is significant here is that an iterative best-fit computer scheme would require in excess of 1.5 million operations per iteration of the 22 possible variables. Unless the values of the unknowns are known to a reasonable degree prior to iteration, this scheme would require a great deal of computer time.

The second problem is interpretation of the results. The calculated spectrum would represent the sum of 288 Lorentzian peaks. Intuitively, one feels any spectrum could be fit using this many peaks.

Simplified Model. Fujita also describes a simpler model

applicable to substitutional solid solutions. In this model, the effects of the second neighbors are assumed to be negligible; and a random distribution of solute atoms are assumed to exist in a closely packed substitutional solution. The atoms are treated as hard spheres of equal diameter packed to near maximum density. The resulting structure yields 12 nearest neighbor atoms. Fujita develops the probability of finding a given combination of atoms, assuming that only two types are present. The probability is

$$P(nA, mB) = {}_{12}C_n c^n (1-c)^m, \quad n+m=12 \quad (2)$$

where  $n$  is the number of atoms of species A,  $m$  is the number of species B,  $C$  is the binomial coefficient for 12 items taken  $n$  at a time, and  $c$  is the concentration of species A. These definitions apply to Eq (1) as well. With the probabilities defined in this manner, the intensity at the calculated spectrum can be described by

$$I(x) = \sum_{n=0}^{12} \frac{\pi A}{\Gamma} {}_{12}C_n c^n (1-c)^{12-n} \frac{1}{1 + [(x - x_0 - \delta_n)/\Gamma]^2} \quad (3)$$

where  $A$  is the total absorption intensity,  $x_0$  is the peak position with no foreign neighbors,  $\delta_n$  represents the line shift due to one foreign neighbor, and  $\Gamma$  is the half width at half maximum of the calculated Lorentzian. Using Eq (3), the calculated spectrum is the sum of 12 Lorentzian peaks.

The contribution from each site is a single peak spec-



trum, which is not what is expected from an iron-rich alloy, nor is it consistent with the results of previous work. Several final assumptions and modifications are required.

Final Model. The first modification to Eq (3) is based on the assumption that the contribution from each site will be a six peak spectrum similar in form to that produced by natural iron, and describable by the simplified Hamiltonian, as developed by Wertheim (Ref 9:72-83). This assumption is based on the results of Tsuei and Fujita, and is considered to be a valid one. The remaining assumptions determine which terms of the final expression [Eq (4)] shall be considered variables.

The first assumption is that each of the sites shall have its peak intensities in the same ratio, but that ratio will not be fixed. If the spins in the material were randomly oriented, a ratio of 3:2:1:1:2:3 for the six peaks contributed by each site would be expected. Tsuei's results indicated a peak ratio other than this, and therefore the simplified model of this study was designed to allow arbitrary variation of the peak ratios. The arbitrary decision to require the peak heights of each site to be in the same ratio was made to simplify the model by reducing the number of variables for peak height from 72 to 6. Note that this scheme does not require symmetrical peaks to be of the same intensity.

The second assumption is that linewidth is an arbitrary



variable. The model was designed to allow three values of linewidth to vary without restriction. Each of the three represents a pair of symmetrical peaks (e.g. peak 1 and peak 6) for a given combination. Each of the combinations is required to have the same linewidths, again an arbitrary decision to increase simplicity and decrease the number of variables. While the assumption does simplify the model, it is unreasonable in the sense that the model allows two symmetrical peaks to vary independently in amplitude, yet requires each to have the same full width at half maximum. If the experimental data is in the form of an asymmetrical pattern, the values found by the least-squares minimization program will represent only a weighted average, and not the best possible fit.

The third assumption is that the contributions from the six least prominent combinations could be neglected. This assumption was made to reduce execution time of the curve-fitting program, and should introduce minimal error into the results. The weighting function for the sixth most prominent combination is 0.0532, and the sum of the contributions from the six remaining combinations is 0.0193.

The final assumption is that the constituent atoms of the materials to be analyzed can be treated as iron and non-iron. This implies that the shift in energy levels of the absorber nucleus is independent of the type of atom interacting with the absorber -- which is contradictory to previous results with Mossbauer spectroscopy, but does allow use of the bi-

nomial distribution. The validity of this assumption is further discussed in the Conclusions.

The final form of the model is then

$$I(x) = \sum_{n=0}^{12} \sum_{m=1}^6 \frac{A_m}{\Gamma_m} 2C_n c^n (1-c)^{12-n} \frac{1}{1 + [(x-x_0 - \delta_0 n)/\Gamma]^2} \quad (4)$$

with the restrictions on variables as noted in the assumptions.

### III. Equipment and Procedures

As a secondary purpose of this study, the existing Mossbauer spectroscopy equipment was modified to simplify use and adjustment and to improve resolution. This chapter will describe the equipment used in data acquisition, as well as the modifications to that equipment. The final sections of this chapter will describe the experimental methods used and the conditions of the data runs.

#### Equipment

The major components of the equipment used were manufactured by Ranger Electronics, and consist of a velocity transducer, a linear amplifier/single channel analyzer, a krypton-filled proportional counter, and a Mossbauer control unit. Additional components consisted of a RIDL 400 channel analyzer, a Wavetek oscillator, a Ranger temperature controller, a heater, a gold (0.07% Fe) - chromel thermocouple, and a digital volt meter. These components are those used by Skluzacek. In his work in 1976, he gives an overall description of the equipment which will not be repeated here (Ref 10: 5-11).

Cryostat and Drive Mechanism. A cryostat, manufactured by Janis, Inc, was used throughout the study with the sample absorber held fixed in a combination heater and mount. The heater/mount and moving source were located near the bottom of the cryostat, and were attached to the Mossbauer drive unit by a 29 inch support and an extension shaft. The

possible problem of a decrease in the rate of change of velocity near zero velocity, as reported by Skluzacek, and a need to simplify the mounting and adjustment of the drive unit, led to the following modifications.

The heater/mount support and motor mount were changed to the configuration indicated in Fig. 1. The changes provided access to the rods forming the support for adjustment, without removal of the motor. These modifications had been initiated prior to the start of this study by Dr. George John, and were completed by the writer.

During reassembly and testing of the modified support and motor mount, two problems were noted: (1) adjustment of the motor extension shaft still required removal of the motor and/or the Mossbauer source; and (2) operation of the motor resulted in a lateral vibration of the extension shaft. It was felt that the vibration was due to the flexibility of the small diameter tube used as the extension shaft. The extension shaft shown in Fig. 2 was designed to replace the existing rod.

The new shaft was constructed of thin wall 1/4 inch diameter stainless steel tubing. The adjustment sleeve was made of aluminum to reduce weight, and the threaded inserts were formed from steel bolt stock center-bored to reduce weight. The source mount was formed from brass rod. The new shaft displayed (visually) none of the tendency to vibrate displayed by the original.

Moire Grating. Skluzacek also reported significant



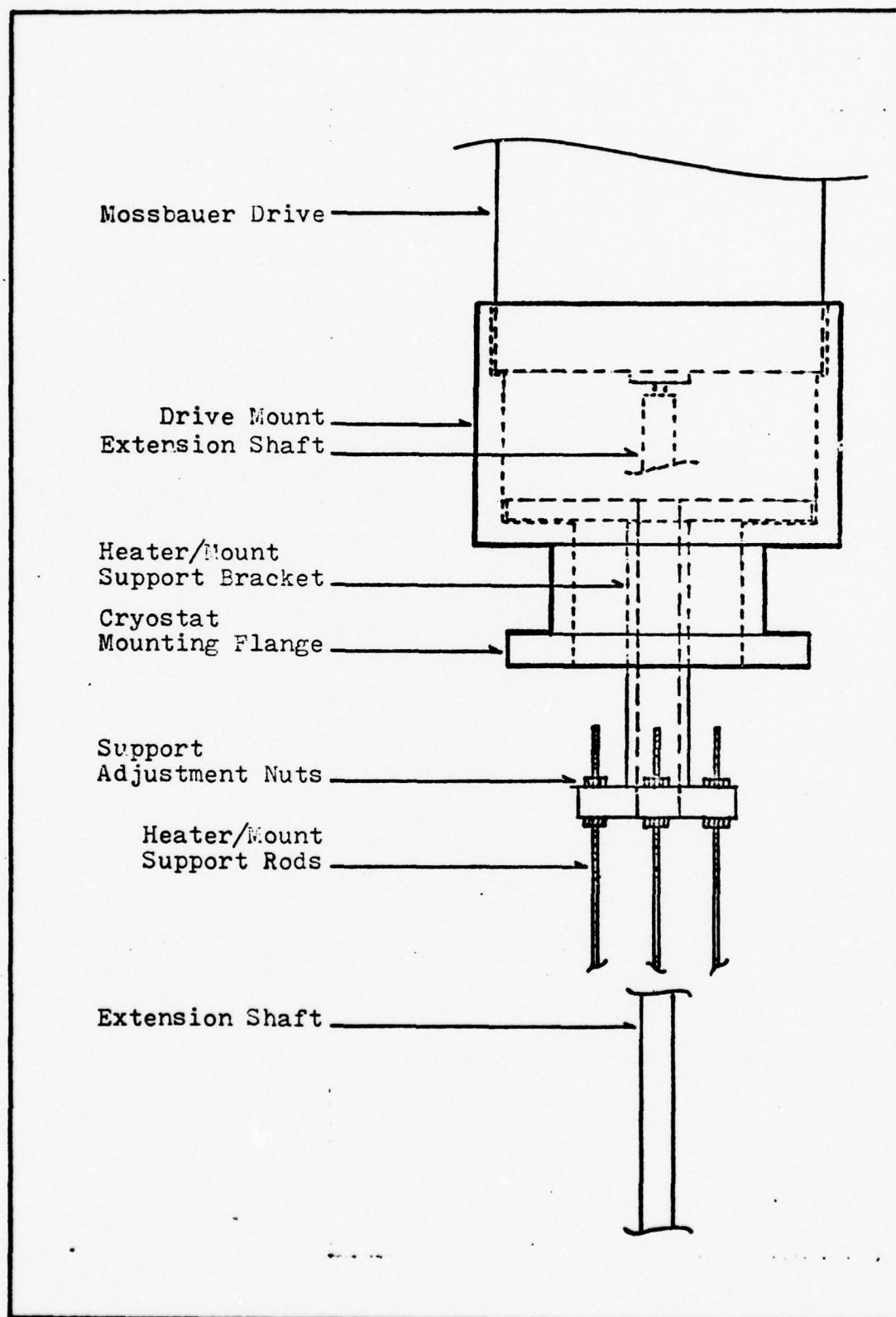


Fig. 1 Modified Motor Mount and Support

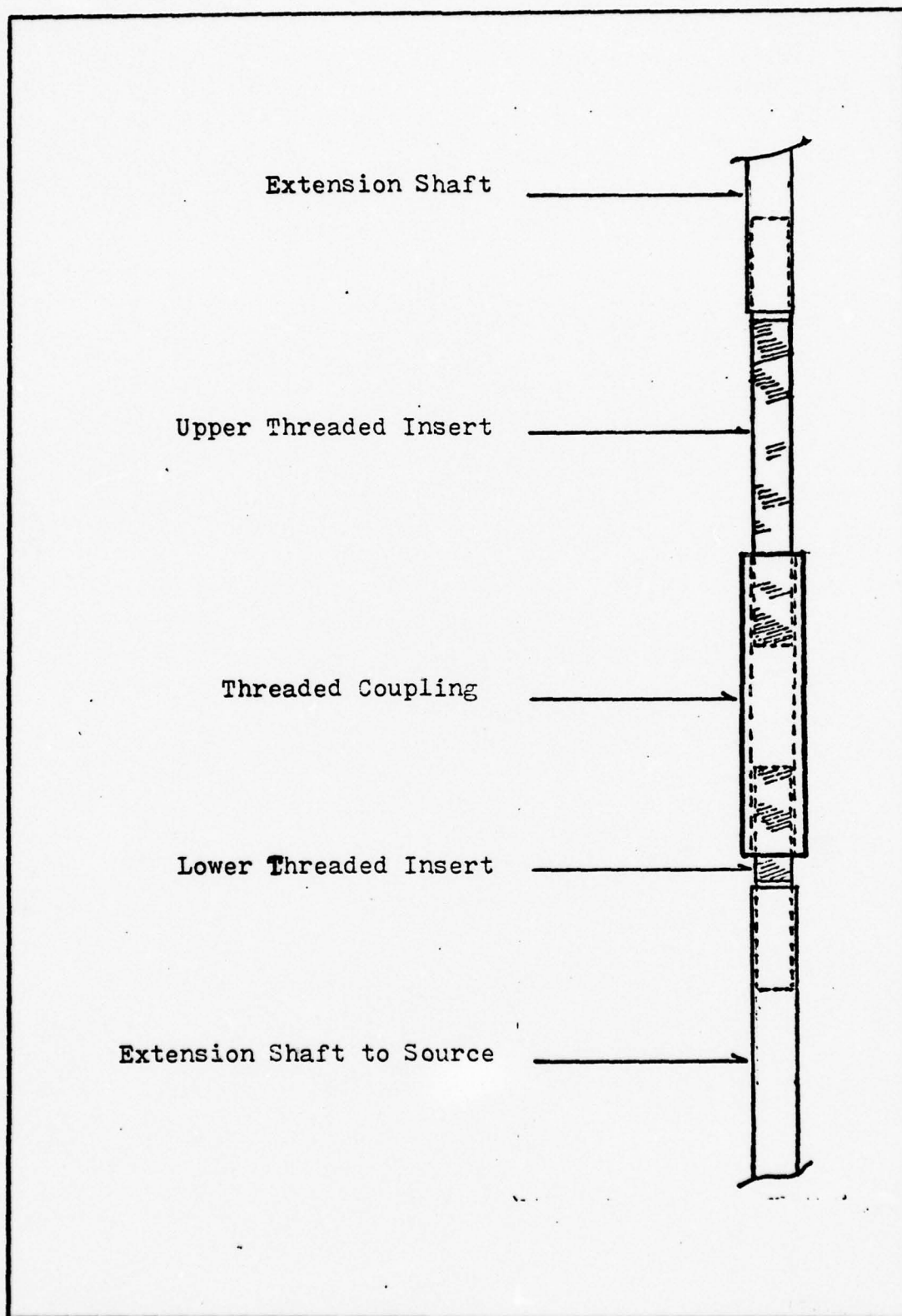


Fig. 2 Modified Extension Shaft

problems with non-linear velocity in the near zero region, due to the use of a high speed Moire grating in the velocity measuring system (Ref 10). Prior to the start of this study, the grating was replaced with one suitable for the velocity range to be used (a maximum of  $\pm 10$  mm/sec). The velocity fits obtained with the new grating and modified extension shaft were typically of  $\pm 0.02$  mm/sec, and were obtained with a first order polynomial fit. A calibration run made with natural iron is described in Chapter IV.

Temperature Control. Data runs were accomplished at both room and liquid nitrogen temperatures. Significant temperature fluctuations were noted at both temperatures. Room temperature runs were accomplished in the cryostat with the vacuum system operating, but large fluctuations in the laboratory ambient temperature resulted in a slow drift of sample temperature through a range of  $\pm 5^{\circ}\text{C}$ .

Runs at liquid nitrogen temperature were initially attempted at a temperature five degrees above the liquid nitrogen reference used for the gold-chromel thermocouple. This was done to avoid fluctuations in temperature while the liquid nitrogen was being serviced, which had been reported by Skluzacek (Ref 10:9). During this study, runs with temperature fluctuations of up to three degrees Kelvin were noted; however, the subsequent failure of the temperature indicating system suggests that the fluctuations may have been the result of the malfunctioning of that system, and not actual variations in the temperature of the sample.

### Source and Absorbers

The source used throughout this study was cobalt-57 in rhodium, prepared by Amersham-Searle. The source was originally of 50 millicurie strength, but had decayed to approximately 16 millicuries at the time of this study.

The absorbers were manufactured by the Batelle Laboratories at Columbus, Ohio, and were made available through Dr. Harold Gegel, of the Air Force Materials Laboratory. A list of the samples examined is given in Chapter V. Each of the samples was manufactured by spin cooling a thin stream of the melt on a cooled rotating drum. All of the samples were similar in form, consisting of thin, narrow strips. Typically these strips were 0.001 inches in thickness and 0.75 mm in width. The thickness showed little variation from sample to sample; however, the width of a given sample would range from 0.50 mm to 1.2 mm. Visual examination of the samples with a binocular microscope showed the edges to be very ragged and the surface to have an irregular pattern generally running the length of the sample.

A simple calculation was made to determine how well the samples matched the conditions developed by Shimony for maximum single line absorption (Ref 11). While the samples were not expected to be single line absorbers, and an optimum thickness would exist for each of the absorption peaks, the calculation of the single line thickness would give an approximation of the actual thickness desired. From Shimony's methods and tables, the calculated thickness was 0.001 inches.



Based on this result, the samples used in this study were formed by using a single thickness of the material.

Twenty  $3/4$  inch strips of the material to be analyzed were placed side by side on ordinary transparent tape, with the strips being placed on the tape in the same orientation that they were cut from the original strip. The samples were formed large enough that the cut, and possible distorted, ends would not be in the zone used for analysis. Similarly, any kinked or distorted portions of the original strip were not used.

In addition to the amorphous alloys, two other absorbers were used for calibration of the system and testing of the curve fitting program: a National Bureau of Standards sodium nitroprusside crystal, and a natural iron foil.

#### Data Collection

As previously noted, each sample was examined at both room and liquid nitrogen temperatures. For each of these runs, the sample was mounted between two 0.75 mm thick disks of boron nitride. This assembly was mounted approximately 1.8 cm from the midpoint of the moving source. After passing through the absorber and disks, the radiation passed through two mylar windows in the cryostat, and entered the detector through a beryllium window. The total absorber to detector distance was 18 cm. The arrangement is shown in Fig. 3.

Collection times for the various runs ranged from 25 to 67 hours, with an average collection time of 50 hours. Ex-

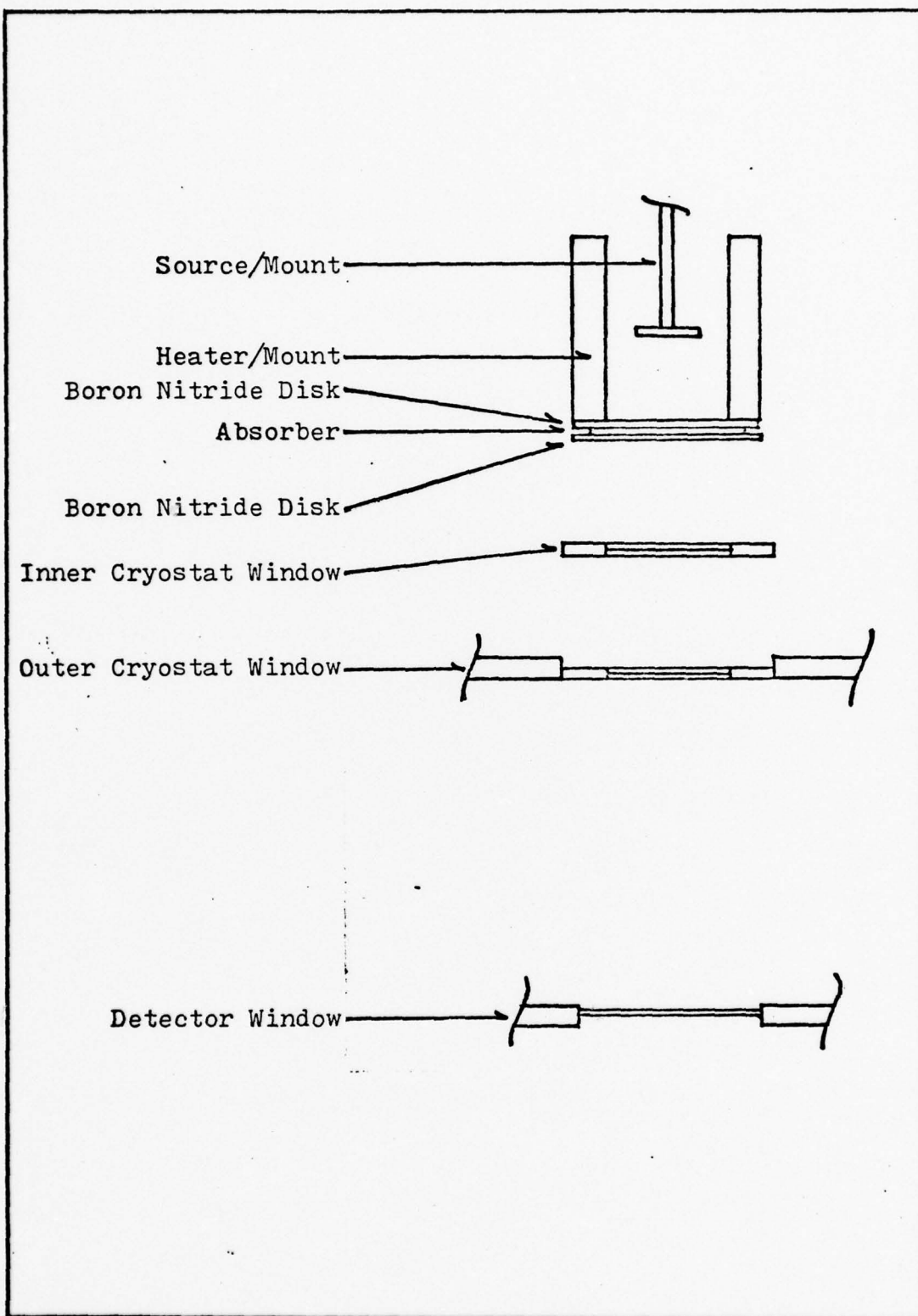


Fig. 3 Experimental Arrangement

perimental conditions during the runs were not consistent. A malfunctioning heating system in the laboratory caused ambient temperatures to vary as much as 15° C during the runs.

Several sources of vibration were present during the runs. The vacuum system used consisted of a fore pump and an oil diffusion pump, both of which were operated continuously during the data runs. The vibration generated by these pumps was transmitted to the cryostat through the required connections. Both of the connections used were rigidly fixed prior to reaching the cryostat, but vibration could still be felt when the pumps were operating.

It can be assumed that both the temperature fluctuations and the vibrations contributed to loss of intensity and to line broadening. The extent of these effects has not been evaluated. It can be assumed that the contribution of vibration will be relatively consistent throughout the runs; however, the effects of temperature changes may be both material and site dependent, and are therefore much more difficult to account for in the spectra.

#### Data Processing

Raw data collected and stored in the multi-channel analyzer consisted of time-base oscillator counts in channels 0 to 15, velocity data in channel 8 and every tenth channel thereafter, and the obtained spectrum in the remaining channels. After completion of a data run, the counts in the first 70 channels were recorded by an automatic typewriter for run identification. The entire spectrum was then recorded on

paper tape with a Tally paper tape punch. The paper tape was converted to Hollerith punched computer cards by use of a permanent library program. Initial processing consisted of the calculation of the velocity curve and the generation of a counts vs. velocity plot. Further processing of the data was made using the GENFIT program, and is discussed in Chapter IV.



#### IV. Data Analysis

The experimentally obtained data was analyzed using a least-squares minimization curve-fitting program originally developed by the Argonne National Laboratory. This program, named GENFIT, requires a user-supplied subroutine to describe the spectrum being analyzed. The GENFIT program varies those parameters specified by the user to obtain the best least-squares fit. The parameters used in this study are those described in Chapter II, which determine the position, width, and height of the absorption peaks generated by each combination of atoms. Numerous changes to the GENFIT program and the READIN subroutine were made to simplify use and to eliminate those portions not applicable to Mossbauer spectroscopy. These changes are described in Appendix A.

The user-supplied subroutine, called CALFUN, provides the means by which the analyst implements an assumed model. This chapter will discuss the program GENFIT, the subroutine CALFUN, the criteria used for goodness-of-fit, and finally, the techniques used in the employment of the program.

##### Program GENFIT

The program GENFIT was modified during this study to add a line-printer plotting capability and, as noted, to simplify its use. The portions of the program performing the actual minimization were left essentially unchanged. The subroutine READIN, written by Skluzacek, was modified to accommodate a change in the channel numbers used for multiplexed velocity

data, and to allow for partial overflows in the data spectrum. A listing of the GENFIT main program and the subroutine READIN is given in Appendix A.

#### Subroutine CALFUN

The subroutine CALFUN is called by the minimization routine to describe the spectrum being calculated. To reduce the execution time of the program, the simplified Hamiltonian, as well as the binomial probabilities, were reduced to numerical values, and used as constants wherever possible.

The subroutine used a total of 17 variables to implement the model described in Chapter II. The required variables were:

1. Baseline: the average number of counts in the background spectrum.
2. Magnetic field: six values describing the internal magnetic field for each of the combinations.
3. Total intensity: total absorption intensity divided by  $\pi$ .
4. Isomer shift: self explanatory.
5. Linewidth: three values describing the full width at half maximum, one each for peaks 1-6, 2-5, and 3-4.
6. Ratios: five values representing the ratio of a given peak to the height of peak six.

A listing of the subroutine CALFUN is included in Appendix B.

#### Goodness-of-Fit

Two criteria were used to measure the goodness-of-fit

obtained by a given computer run. One of these was objective (Chi-squared), and the other subjective (the visual appearance of the calculated spectrum). These criteria were primarily used to compare the results of various computer runs, and only provide a secondary indication of the validity of the model.

A value of Chi-squared was generated by the GENFIT program and differs slightly in definition from that normally used. Because the total number of data points considered in each of the spectra varies slightly, the value of Chi-squared is defined by

$$\text{Chi}^2 = \frac{(\text{data point}_i - \text{calculated point}_i)^2}{\text{data point}_i} \quad (5)$$

The subjective criterion of visual appearance was required because of the program GENFIT's tendency to "lock in" to local minima, rather than to absolute minima. In these cases, the calculated spectrum could have a reasonable value of Chi-squared, and yet bear little resemblance to the experimental data. In such cases, the visual appearance of the generated plots was the controlling criterion.

#### Use of the Program

The use of a model which forced a binomial distribution on the contributions of each combination allowed a simpler means of analysis than would have been possible with free variation of the contributions. The plot of counts vs. vel-

ocity obtained in initial processing was used to determine approximate values for the various parameters. For example, the site or combination having the greatest contribution would be assumed to have an internal magnetic field such that its peaks one and six would fall directly under peaks one and six of the experimental peaks. Using similar methods, and assuming a distribution of values proportional to the percent of iron present at a given site, a reasonable estimate for each of the parameters can be found.

The initial run of the program GENFIT was made using a very limited number of iterations, and without requiring convergence. The results of this run allow the detection of any gross errors in the initial estimates, as well as disclosing any singularities in the values. It was noted in the data analysis that certain combinations of values "trap" the minimization scheme in a non-converging iteration of values.

Once the initial values have been confirmed or modified by these short runs, successive runs can be made using the results of the previous run. Two exceptions exist to this general rule. The first is the use of the variable called baseline. The minimization scheme treats baseline as a free variable, although it represents the value of the average number of counts in the background spectra. It is recommended that this value be calculated manually, and that this value be used for all computer runs of that spectrum. The second exception occurs when the calculated spectrum deviates significantly from the experimental. Normally, in these



cases, the program has "locked in" to a local minimum, and it is necessary to adjust manually one or more of the parameters away from the program generated value and re-execute the program.

Further comments on the use of the program GENFIT can be found in Ref 10.

## V. Results

The Mossbauer pattern obtained for each of the materials analyzed and the best-fit calculated spectrum are shown in Figs. 4 to 17 in this chapter. Each of the calculated spectra were generated using the model described in Chapters II and IV. Table I presents the values obtained for the 17 parameters used in the curve fitting, as well as the conditions of each run.

Runs are identified by sample composition, followed by a run number. For example, FE80B20 #2 would be the second run with a sample composed of 80% iron and 20% boron.

### Certainty

Uncertainty values for the parameters listed in Table I are not listed, in order to reduce confusion in the table. In addition, the magnitude of the uncertainties is primarily a function of the computer time allowed for the program to converge to a minimum least squares. A list of the typical values of uncertainty for each of the variables is included here, and represents the worst values found.

For internal magnetic fields, the value was typically  $\pm 0.5$  kOe for the five largest fields; for the smallest calculated field, the value was typically  $\pm 2.5$  kOe. For line-widths, the value was typically 0.01 mm/sec or less. Isomer shift values were  $\pm 0.001$  mm/sec, and values for the peak height ratios were  $\pm 0.02$  or less. Other factors relating to the certainty of the calculated values are discussed in Chapter VI.

Table I

Table One summarizes the results of the calculated spectra. Abbreviations used in the table are Temp for temperature in degrees Kelvin, Hfld for internal magnetic field expressed in kOe, Chi Sqd for Chi-squared, LW for line-width, which is followed by the applicable peak numbers, Iso Sft for isomer shift, and Rat for the ratio of the indicated peak height to peak number six. Throughout this report, peaks are numbered from the peak with the most negative velocity as number one, to the peak with the most positive velocity as peak number six.

Table I

## Measured and Calculated Parameter Values

Fig No.	Identification	Temp	Hfld-1	Hfld-2	Hfld-3	Hfld-4	Hfld-5	Hfld-6	Chi Sqd
4	FE80P13C7 #1	300	267	249	212	172	129	91	443
5	FE80P13C7 #3	75	320	299	261	220	170	115	1187
6	FE80B20 #1	300	301	279	256	234	213	189	1925
7	FE80B20 #2	75	336	313	288	263	240	217	3499
8	FE80B20 #3	75	336	313	287	262	239	216	2556
9	FE80P11.7C6.3B2 #1	300	245	263	220	181	136	94	622
10	FE80P11.7C6.3B2 #2	75	322	302	269	233	190	123	611
11	FE80P8.5C4.5B7 #1	75	328	304	275	244	213	191	1239
12	FE80P8.5C4.5B7 #2	300	282	262	235	204	170	106	931
13	FE80P6.5C3.5B10 #1	75	328	305	275	243	205	120	1638
14	FE80P6.5C3.5B10 #2	300	294	272	245	216	182	91	1177
15	FE80P11.7C6.3SI2 #1	75	320	302	270	235	193	134	1037
16	FE80P11.7C6.3SI2 #2	300	247	267	223	183	136	96	648

Symbols and units defined on page 27.



Table I (Continued)

Fig No.	LW 1-6	LW 2-5	LW 3-4	Iso Sft	Rat -1	Rat -2	Rat -3	Rat -4	Rat -5	Rat -6
4	0.82	0.58	0.44	0.078	1.00	1.58	0.61	0.65	1.55	1.00
5	1.03	0.67	0.45	0.079	0.97	1.51	0.69	0.70	1.50	1.00
6	0.52	0.40	0.40	-0.036	0.98	1.39	0.43	0.42	1.33	1.00
7	0.61	0.43	0.40	-0.043	0.98	1.13	0.49	0.47	1.09	1.00
8	0.56	0.39	0.37	-0.046	0.98	1.46	0.47	0.46	1.40	1.00
9	0.91	0.61	0.39	0.063	0.97	1.57	0.64	0.68	1.56	1.00
10	0.94	0.70	0.45	0.064	0.99	1.16	0.68	0.66	1.16	1.00
11	0.77	0.56	0.47	0.038	0.99	0.59	0.58	0.56	0.57	1.00
12	0.75	0.59	0.41	0.034	0.98	1.48	0.56	0.57	1.45	1.00
13	0.84	0.53	0.40	0.008	0.95	1.31	0.57	0.57	1.29	1.00
14	0.66	0.57	0.45	0.018	0.97	1.51	0.42	0.44	1.47	1.00
15	0.97	0.79	0.51	0.074	0.99	0.68	0.66	0.65	0.67	1.00
16	0.90	0.63	0.42	0.071	0.97	1.53	0.60	0.63	1.50	1.00

Linewidths in mm/sec.

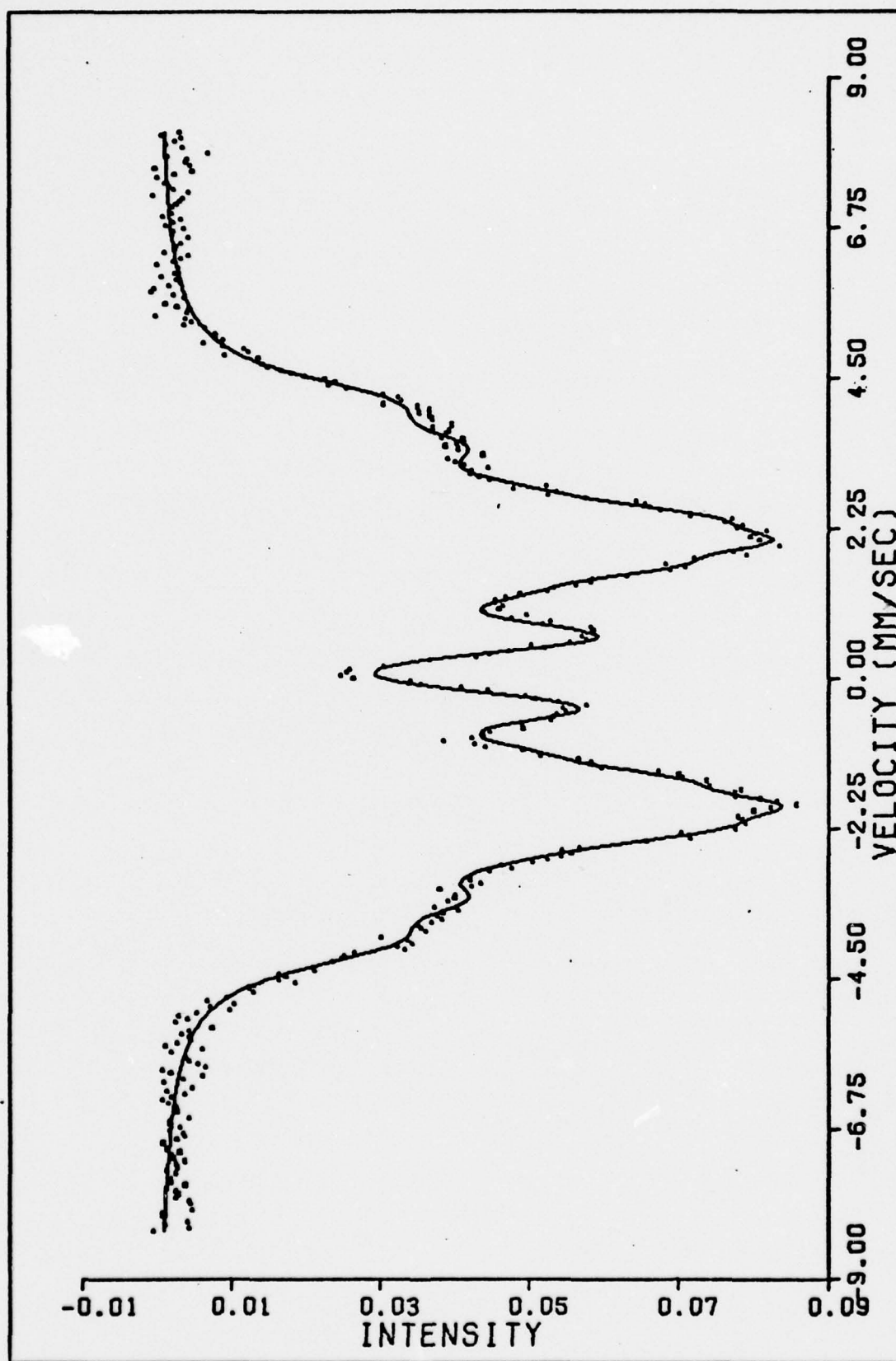


Fig. 4 Mossbauer Spectrum of  $\text{Fe}_{80}\text{P}_{13}\text{C}_7$  at  $300^\circ\text{K}$

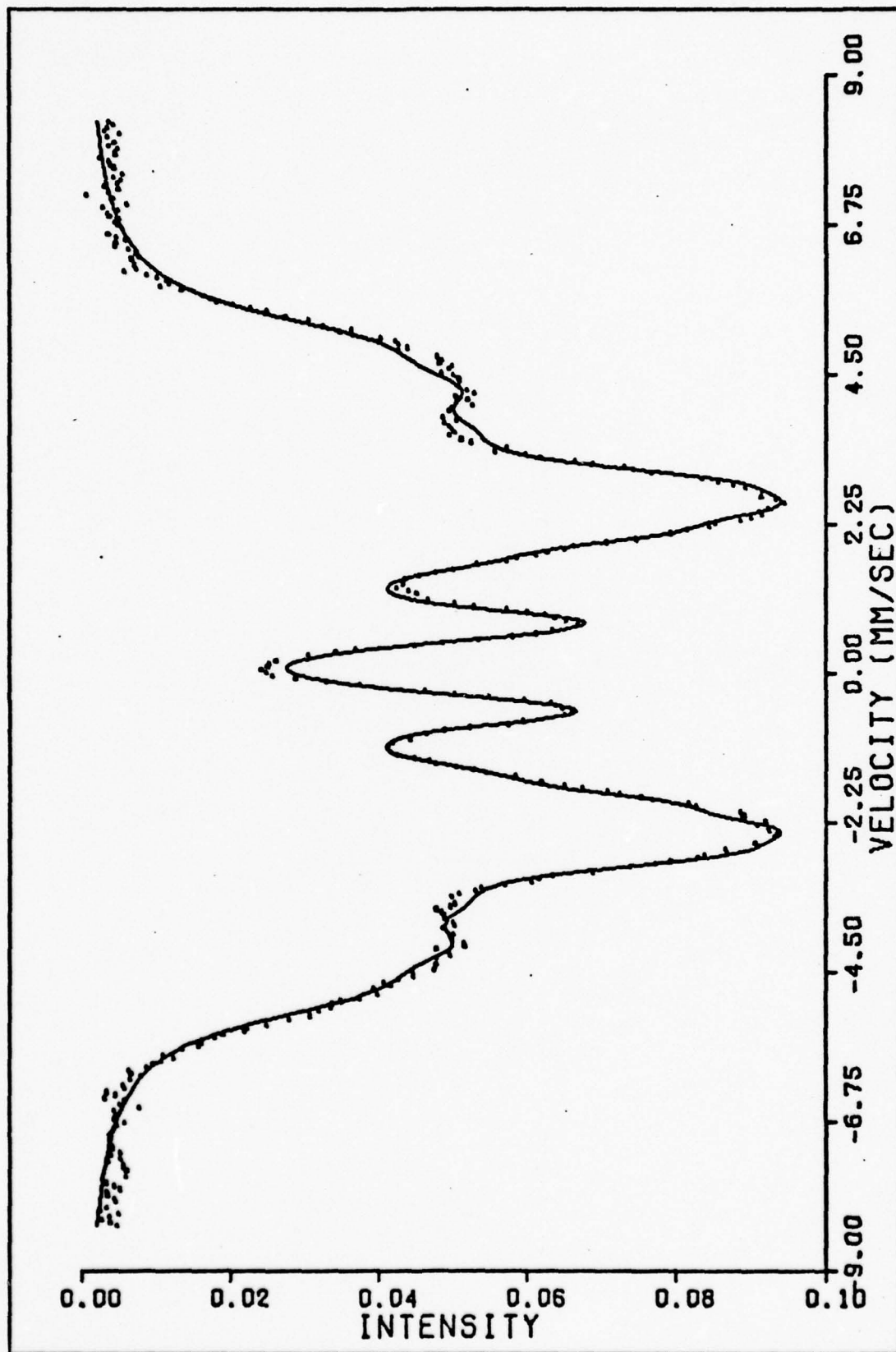


Fig. 5 Mossbauer Spectrum of  $\text{Fe}_{80}\text{P}_{13}\text{C}_7$  at  $75^\circ\text{K}$

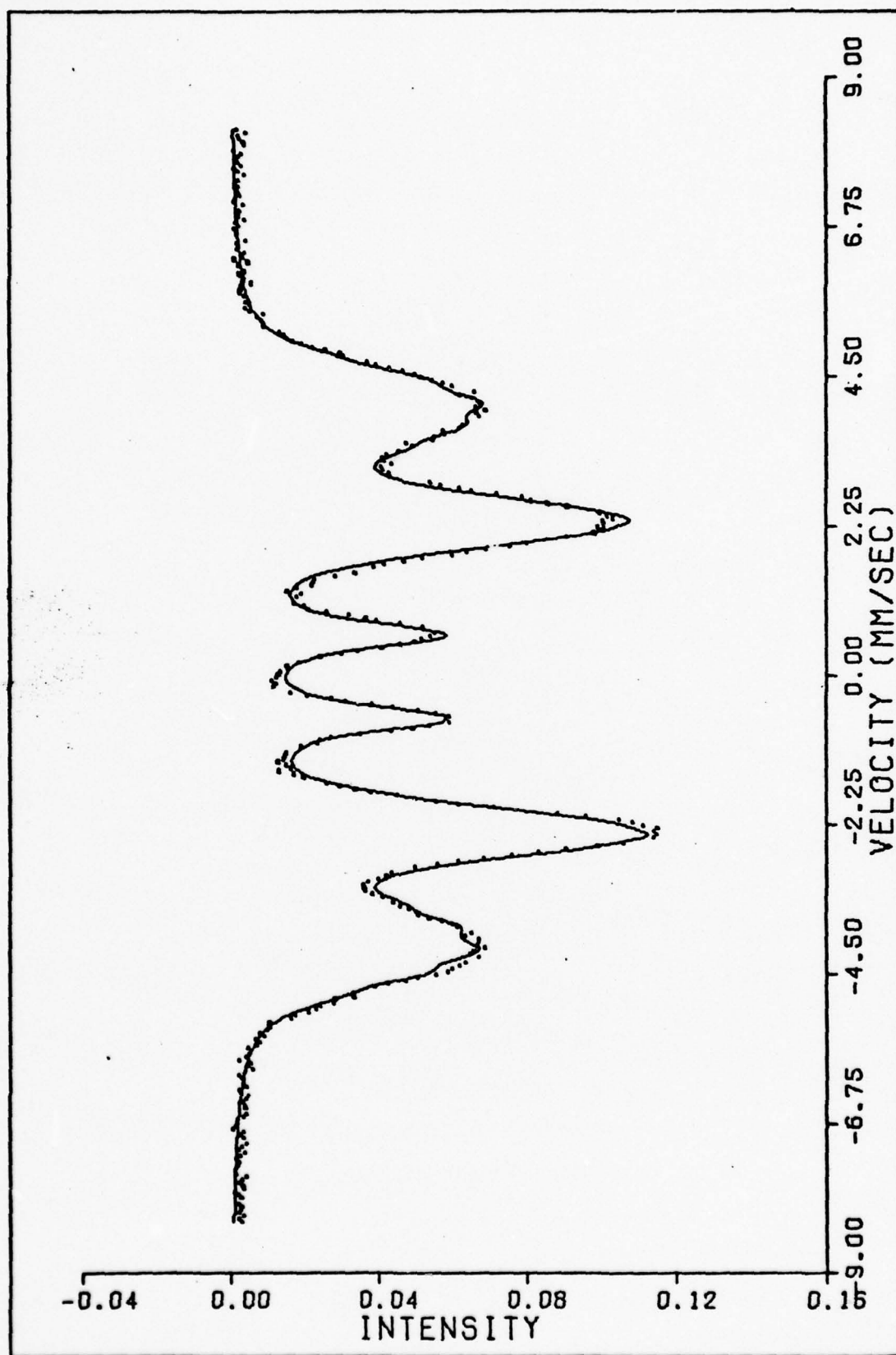


Fig. 6 Mossbauer Spectrum of Fe<sub>80</sub>B<sub>20</sub> at 300°K



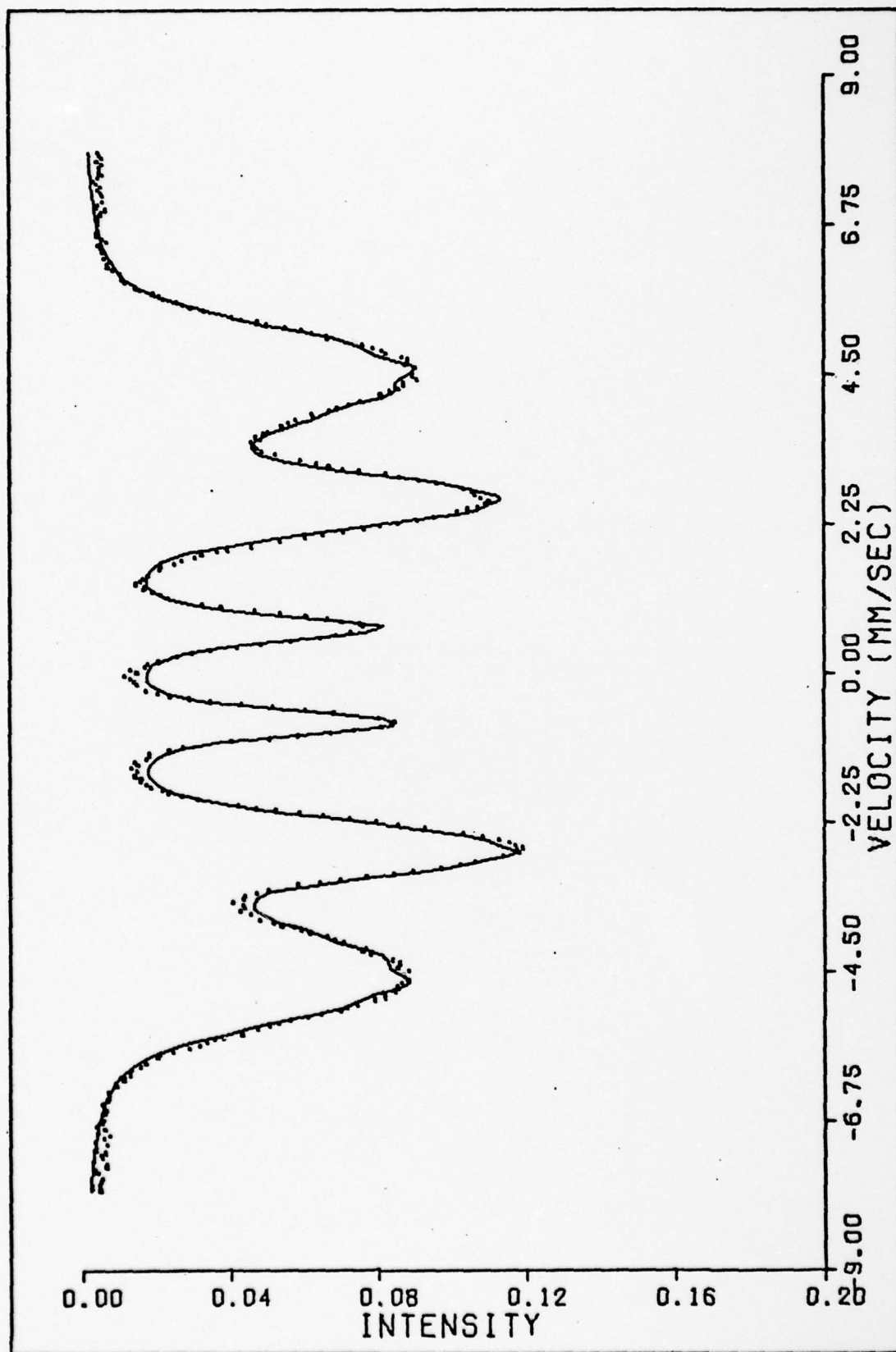


Fig. 7 Mossbauer Spectrum of Fe<sub>80</sub>B<sub>20</sub> at 75°K

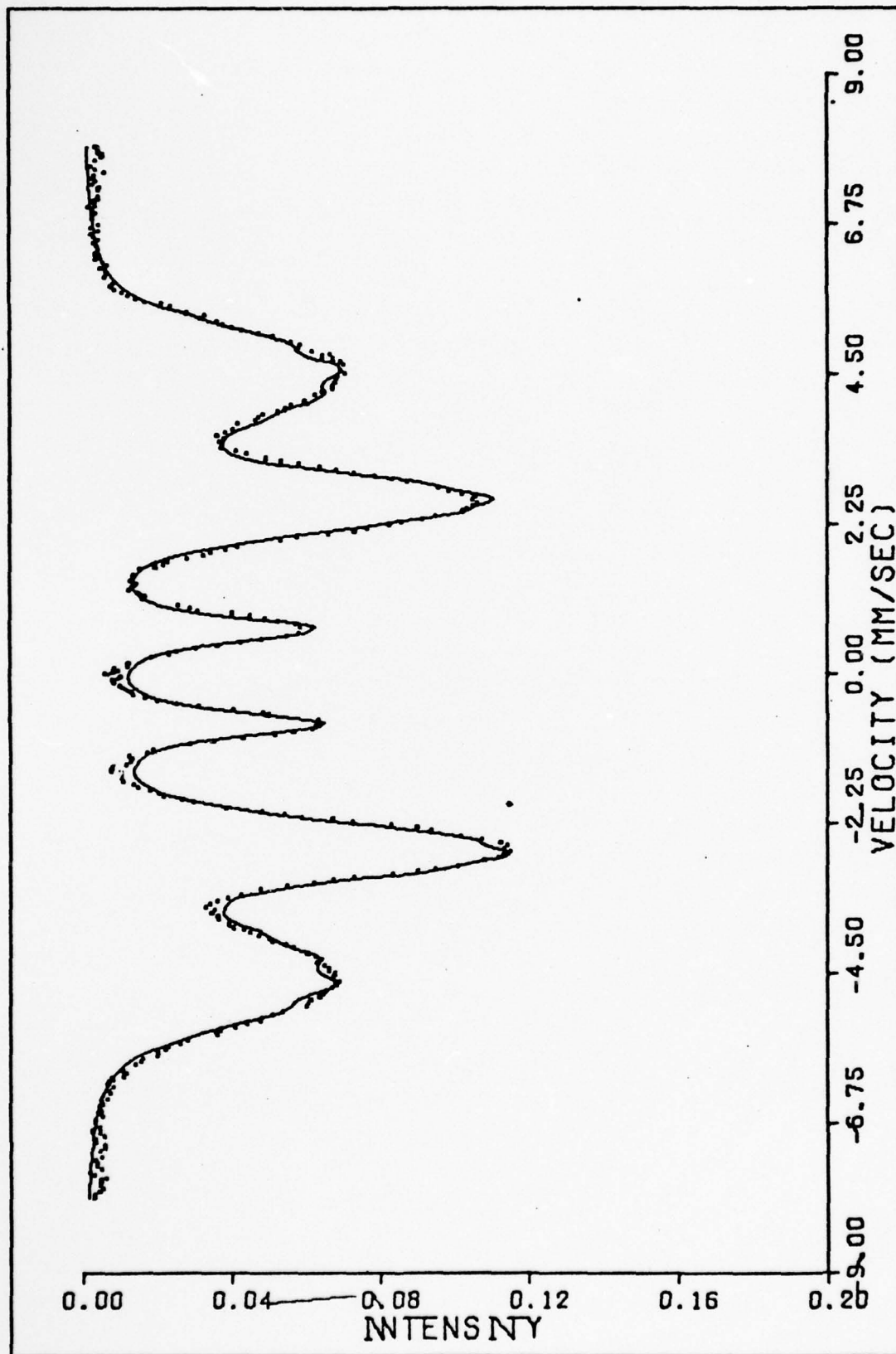


Fig. 8 Mossbauer Spectrum of  $\text{Fe}_{80}\text{B}_{20}$  at 750K (Degaussed)

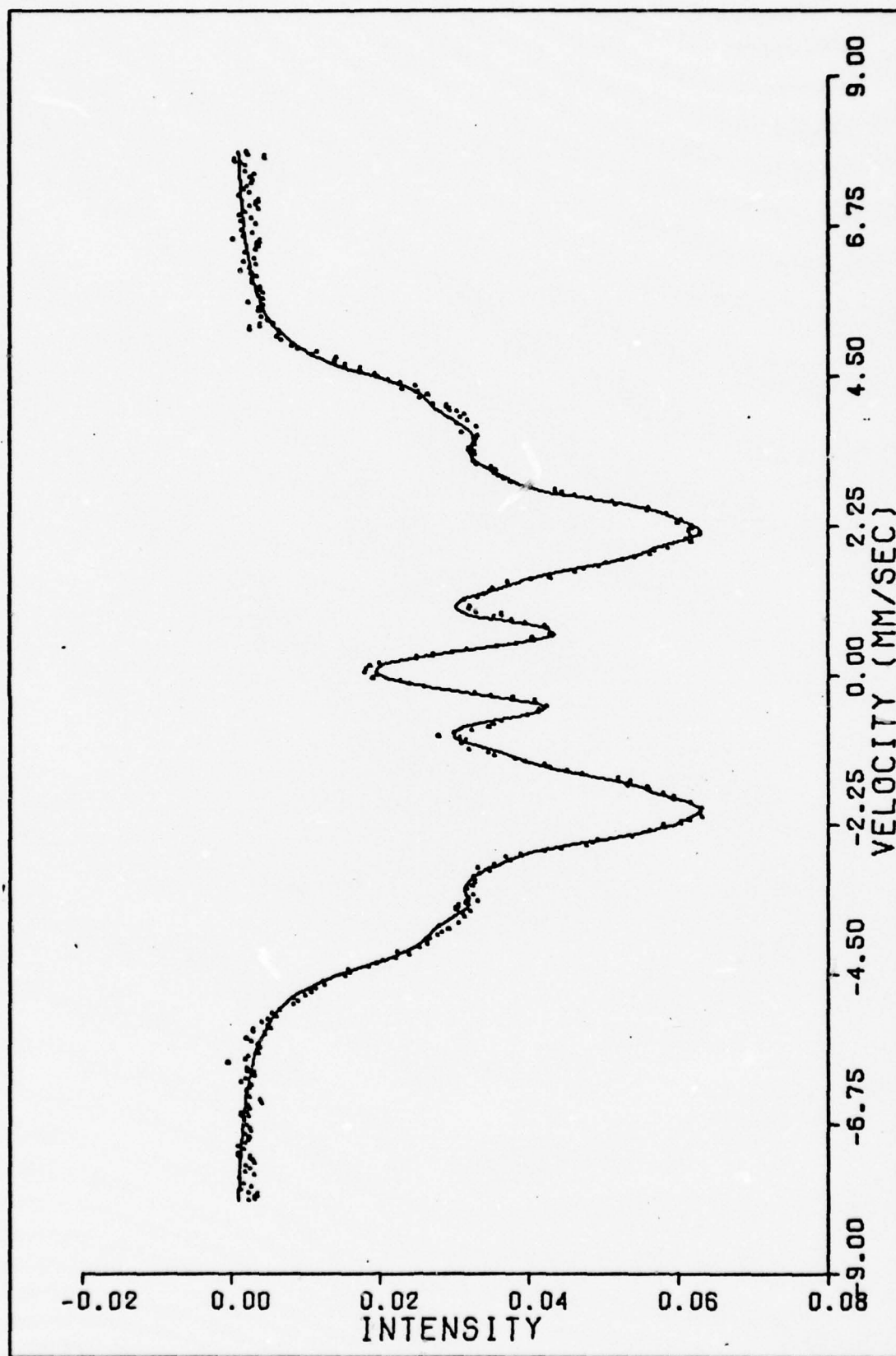


Fig. 9 Mossbauer Spectrum of  $\text{Fe}_{80}\text{P}_{11.7}\text{C}_{6.3}\text{B}_2$  at 300°K

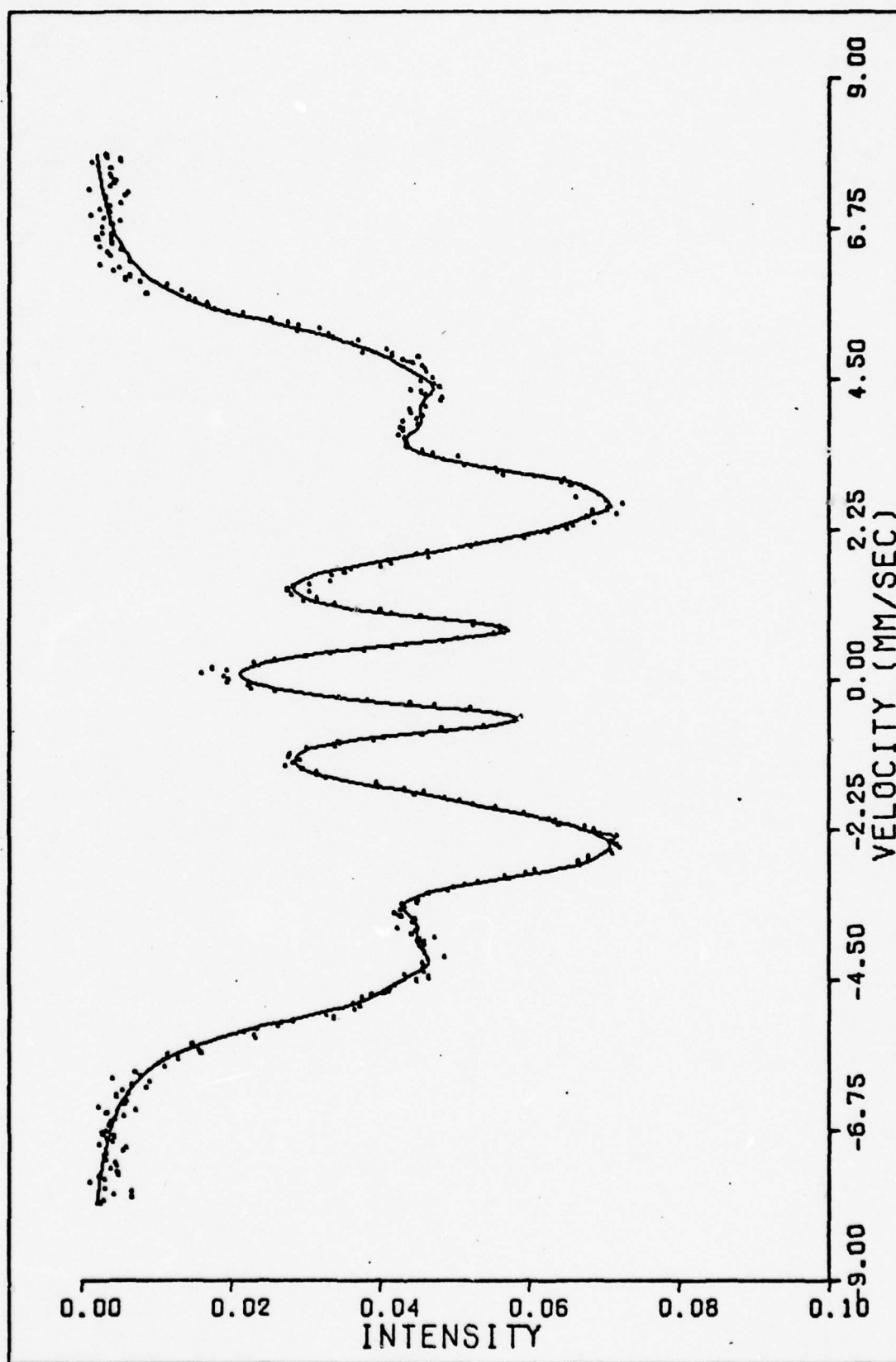


Fig. 10 Mossbauer Spectrum of  $\text{Fe}_{80}\text{P}_{11.7}\text{C}_{6.3}\text{B}_2$  at  $75^\circ\text{K}$



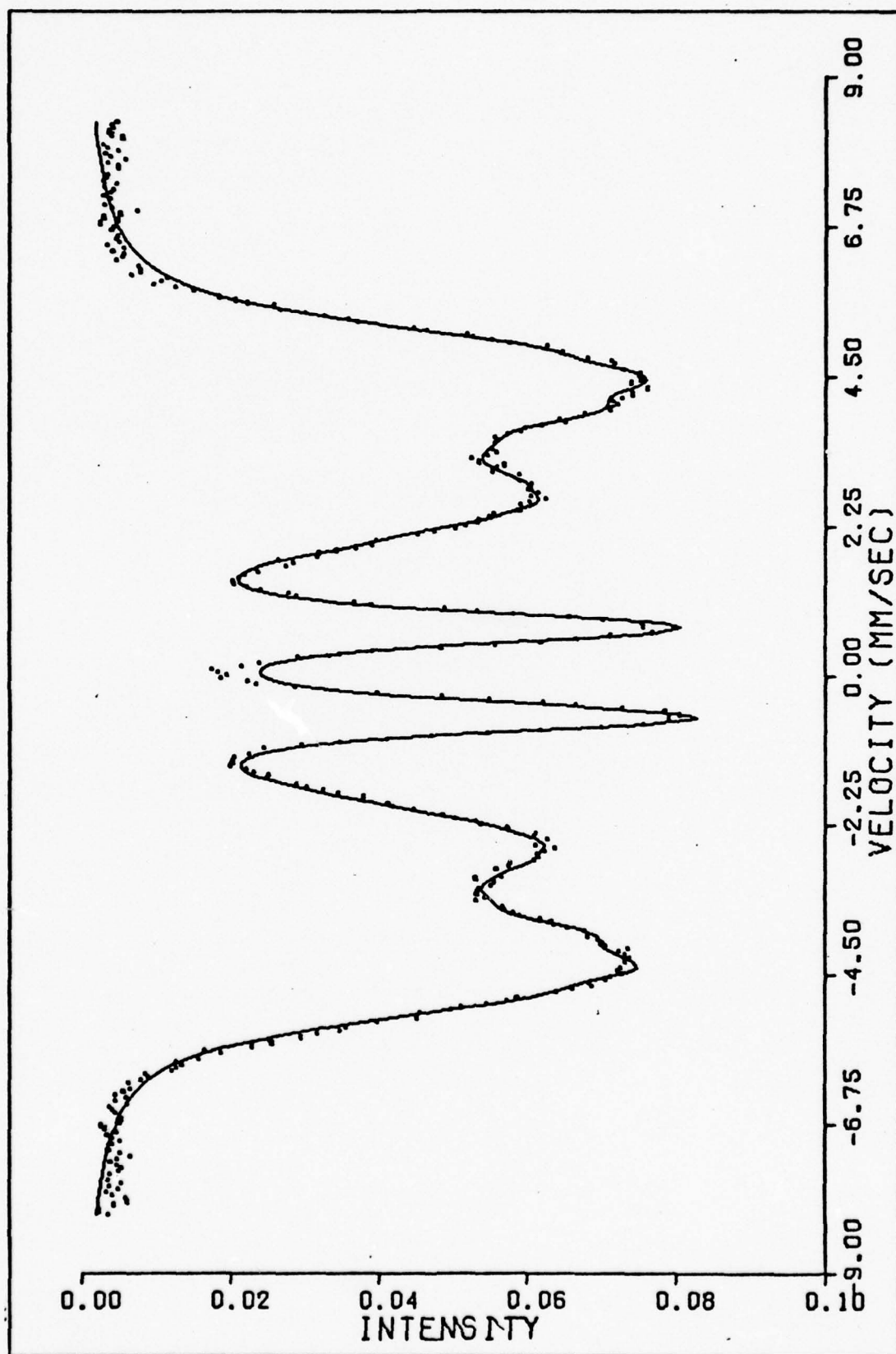


Fig. 11 Mossbauer Spectrum of  $\text{Fe}_{80}\text{P}_{8.5}\text{C}_{4.5}\text{B}_7$  at  $75^\circ\text{K}$

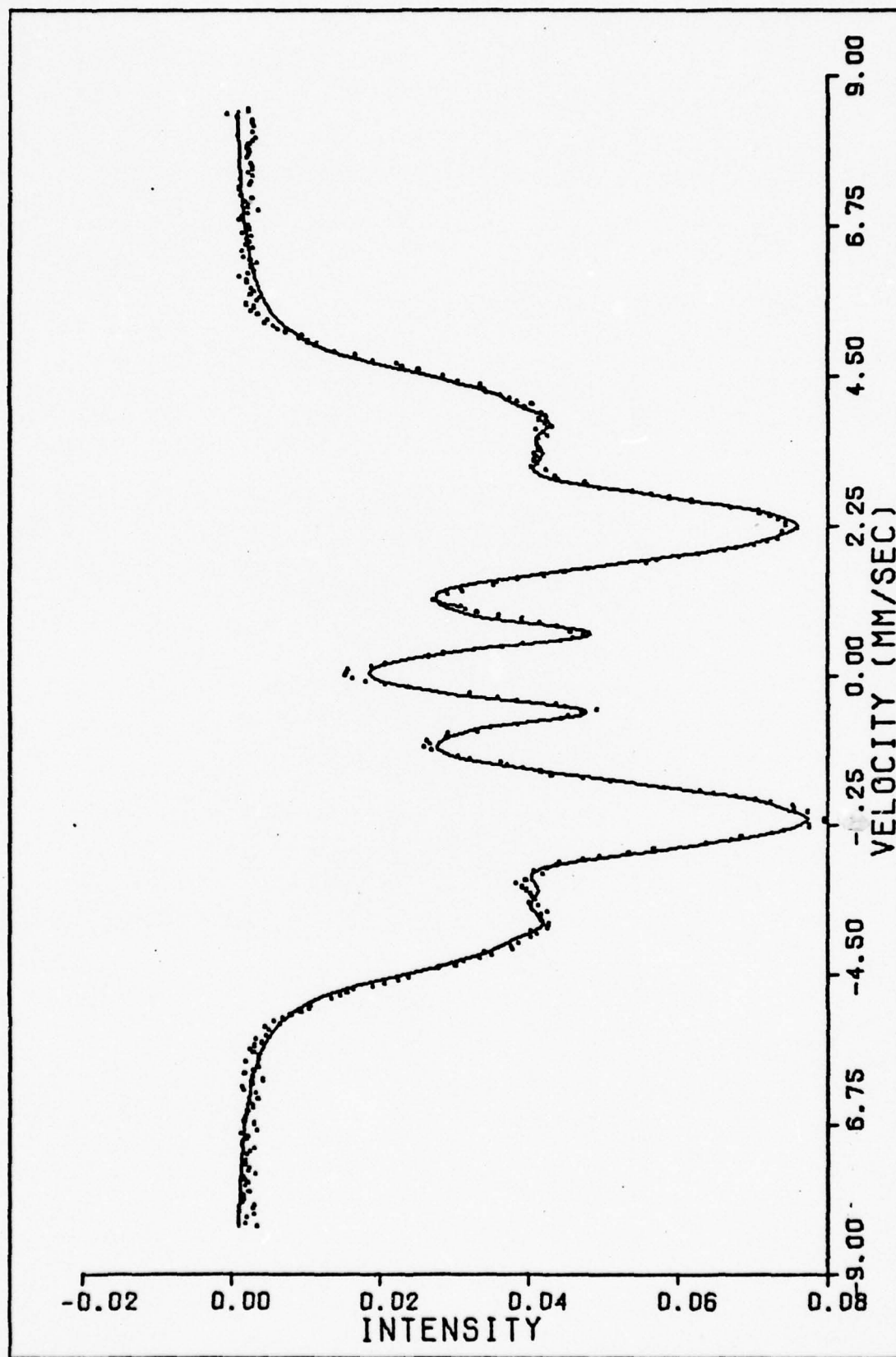


Fig. 12 Mossbauer Spectrum of Fe<sub>80</sub>P<sub>8.5</sub>C<sub>4.5</sub>B<sub>7</sub> at 300°K

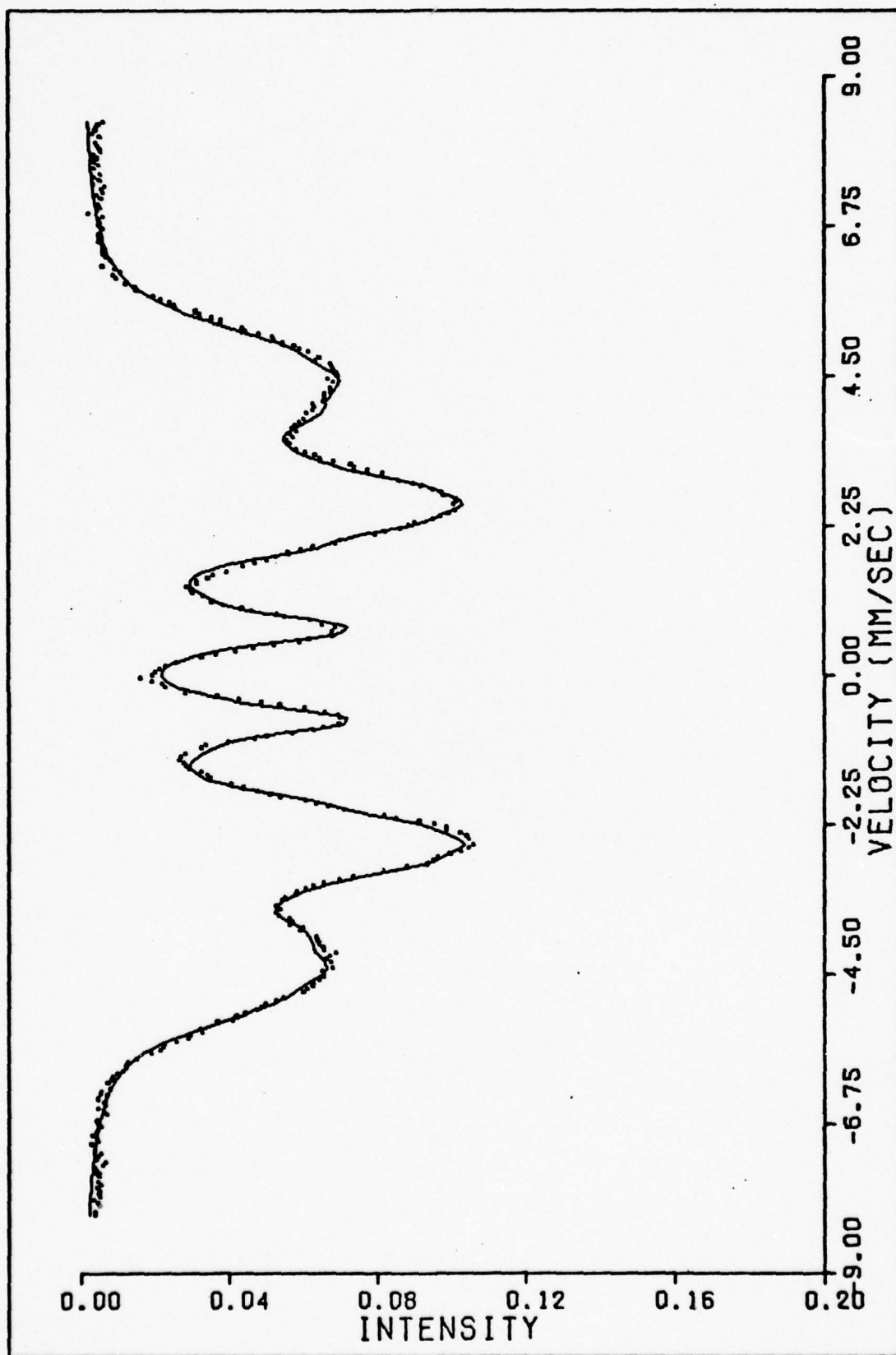


Fig. 13 Mossbauer Spectrum of  $\text{Fe}_{80}\text{P}_{6.5}\text{C}_{3.5}\text{B}_{10}$  at  $75^\circ\text{K}$

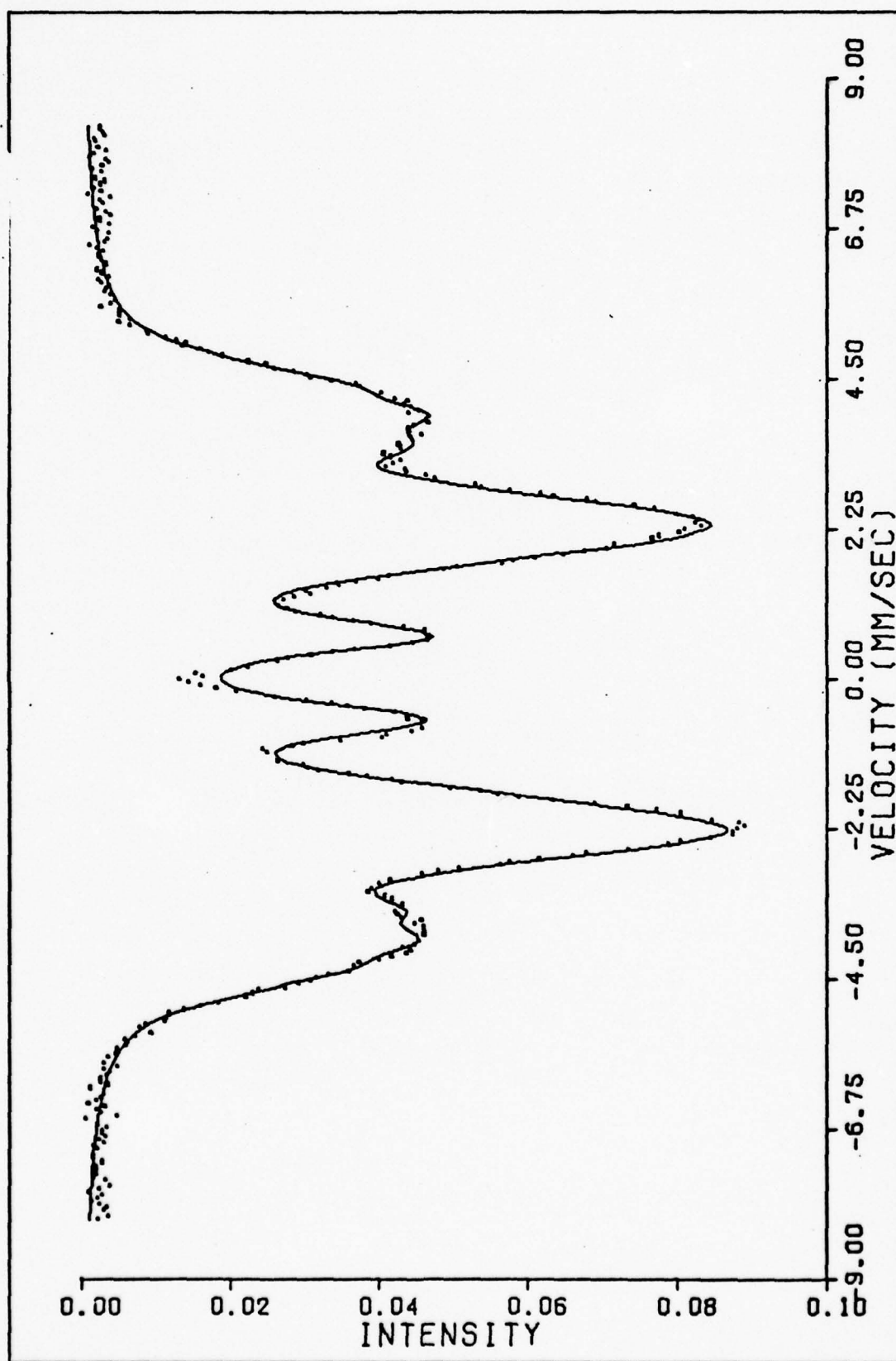


Fig. 14 Mossbauer Spectrum of  $\text{Fe}_{80}\text{P}_{6.5}\text{C}_{3.5}\text{B}_{10}$  at  $300^\circ\text{K}$



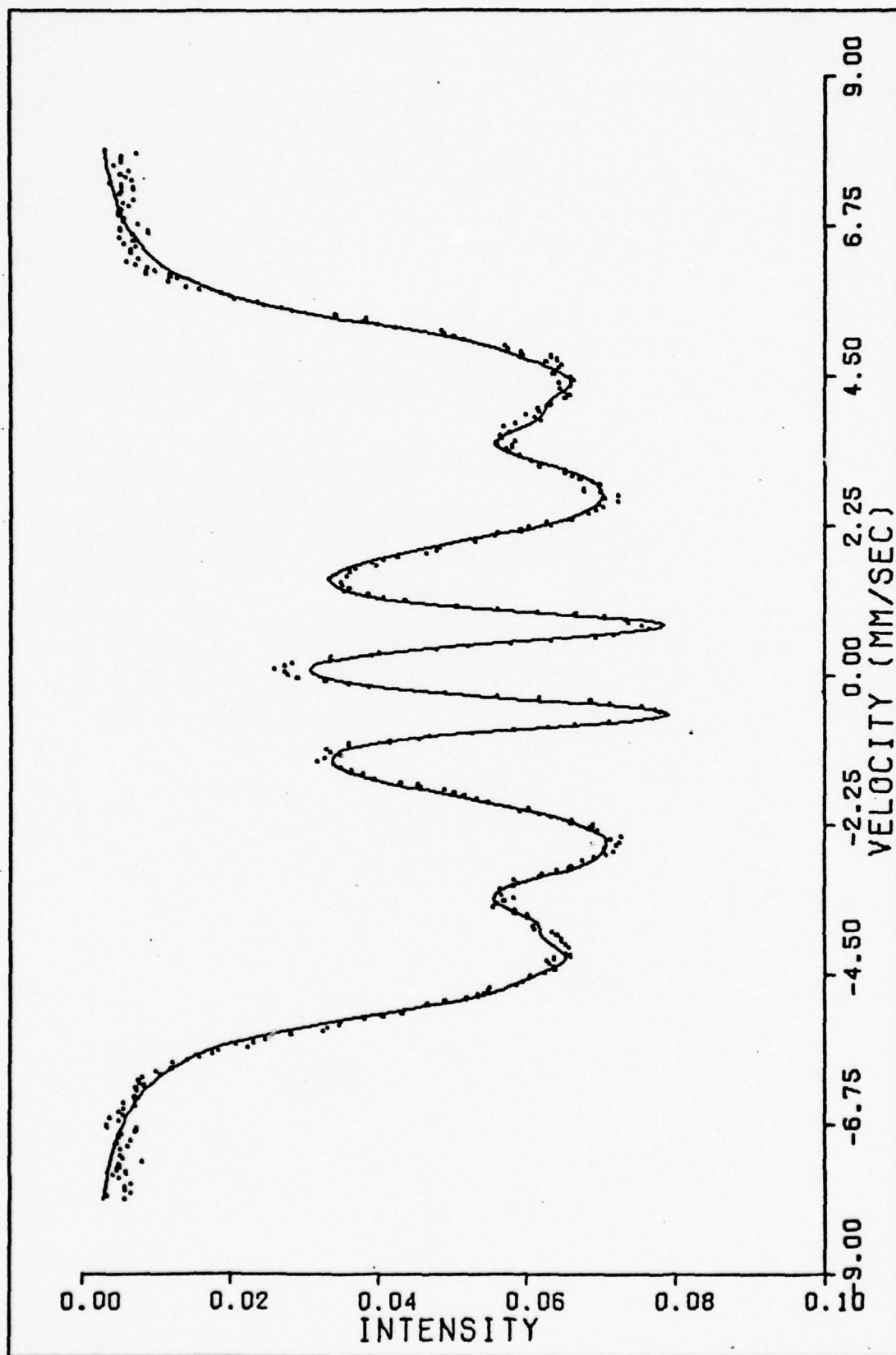


Fig. 15 Mössbauer Spectrum of  $\text{Fe}_{80}\text{P}_{11.7}\text{C}_{6.3}\text{Si}_2$  at  $75^\circ\text{K}$

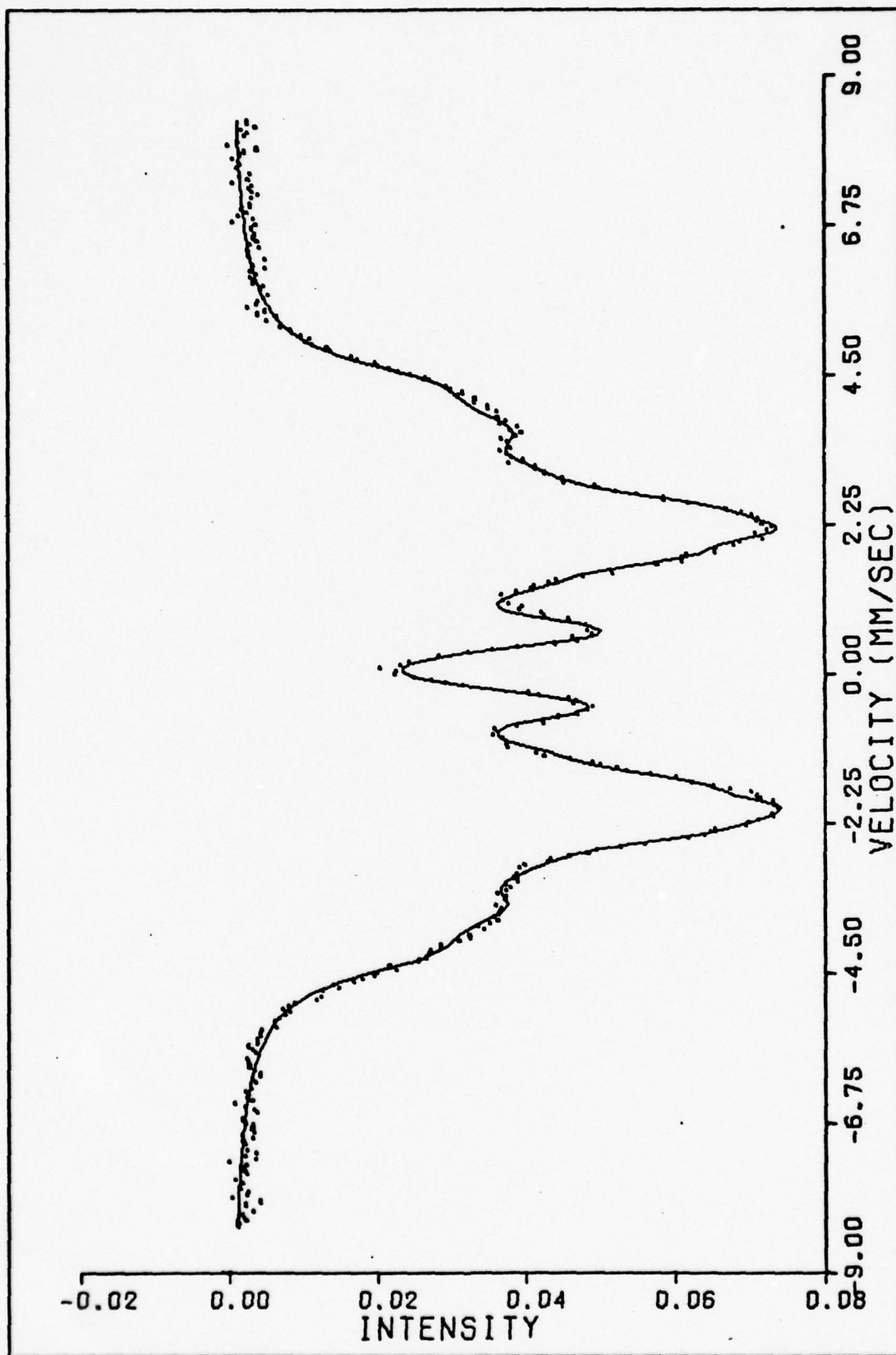


Fig. 16 Mossbauer Spectrum of  $\text{Fe}_{80}\text{P}_{11.7}\text{C}_{6.3}\text{Si}_2$  at  $300^\circ\text{K}$

## VI. Conclusions and Recommendations

The results obtained in this study lead to several conclusions. While the results indicate a general failure of the model in describing the structure of the samples, two notable exceptions will be discussed in this chapter. In addition, several conclusions independent of the model can be drawn. This chapter will first discuss the shortcomings of the model used, the two materials which appear to be exceptions, the conclusions independent of the model, and, finally, will offer several recommendations toward further study of these amorphous materials.

### Structural Model

The use of the substitutional-solid model produced calculated spectra that were generally satisfactory visually. However, the parameter values generated in the curve fitting raise a question as to the validity of the results.

The values of Chi-squared obtained ranged from 443 for the "best" fit to 3,499 for the "worst". If the model were to describe all of the materials adequately, the values of Chi-squared obtained would be expected to have a random distribution over a much smaller range, in the limit approaching the number of data points fitted. The room temperature spectra of the parent material approached this value with a Chi-squared of 443 and approximately 360 data points; however, the same material at 75°K yielded a Chi-squared value of 1,187. This trend was repeated for all except one of the

spectra obtained. The generally high values of Chi-squared and the non-random distribution of values with changed temperature indicate a failure of the model to describe adequately the structure of all the samples. The assumption that constituent atoms could be treated as iron and non-iron is, as anticipated, invalid.

Significant here, however, are the results obtained with  $\text{Fe}_{80}\text{B}_{20}$ . Here the constituents are iron and non-iron, and the probability of a site being occupied by either iron or boron should follow a binomial distribution. Yet the results obtained were not the best obtained; in fact, these were the highest values of Chi-squared obtained. This discrepancy could be explained if the iron-boron compound acted in the manner described by Fujita for a body centered cubic iron-rich compound (for which second neighbor effects are not negligible), while the more complex compounds formed not only the body centered cubic, but also contained a high percentage of randomly distributed interstitial atoms. The combined effects of an absorber's first neighbors and closest interstitial neighbors might be more nearly described by this study's model than is the binary compound itself.

The values of linewidth and peak ratio generated in the curve fitting process results in a second problem. The values obtained for linewidths are similar to those obtained by Tsuei, ranging from 1.03 mm/sec to 0.37 mm/sec (Ref 8:605). Fujita, using his model, reports values for linewidths "a few tens of percent broader" than that obtained for pure iron



(Ref 6:232). In a calibration run made with natural iron, an average linewidth of 0.24 mm/sec was obtained, indicating that the experimentally obtained linewidths are considerably in excess of a few tens of percent larger than the natural linewidths. The implication is that the values of linewidth were increased by the curve fitting routine in order to "fill" the absorption peaks, and that contribution from more site combinations was required. It is not felt that using more than six of the twelve sites in this model would have improved the values of linewidth. More combinations with nearly equal contributions would be required.

The relative peak heights obtained also indicate a possible problem. If the spins are randomly oriented in the sample, the value obtained for peak height should be in an approximate ratio of 3:2:1:1:2:3. This set of ratios was not obtained with the experimental data. The obtained ratios can indicate a non-random distribution of spins. However, again the question of whether enough combinations were considered to properly describe the spectrum must be considered. The ratios obtained may not be significant.

Evidence exists to suggest that the results obtained are possibly a function of both of these causes. The experimental spectra were not perfectly symmetrical, and the ratios changed significantly with temperature: both suggesting an other-than-random spin in the absorber atoms. On the other hand, allowing the ratios to vary arbitrarily, as well as requiring the ratios of each site contribution to be the

same, places a great uncertainty on the values obtained. The question remains unresolved.

### Exceptions

In those samples containing boron, the percentage of boron increases, and the amplitude of the outermost peaks shows a nearly proportional increase until seven percent boron is reached. Above seven percent, the amplitude decreases. In the seven percent boron sample, the outer peaks have an intensity 0.015 greater than peaks two and five. The two percent silicon sample has a similar distribution of peak heights with the outer peaks only 0.005 less intense than peaks two and five. It is only in these two samples that peaks 2, 3, and 5 show a 1:1:1:1 ratio. These effects are only evident in the runs at liquid nitrogen temperature (Figs. 10, 14).

Two possible causes exist to explain these significant changes in the samples as they are cooled. The first is that there is a significantly different vibrational mode of the resonating atoms, resulting in a change in the relative line intensities of the contributing sites. A second possibility is a different angular dependence of the nuclear Zeeman effect. The first of these possibilities suggests a non-cubic symmetry, and the second suggests a material with a preferred orientation (Ref 12:16). In either case, the results indicate a different structure for these two materials at liquid nitrogen temperature than at room temperature, and as compared to the remaining materials.

### Model Independent Results

The patterns obtained through Mossbauer spectroscopy are only a measure of the effect that surrounding atoms have on the absorber nucleus, and it is conceivable that two different combinations of neighbor atoms could result in the same Mossbauer spectrum. Fujita reports obtaining the same spectra for three different (atomic percentages) iron-phosphorous-carbon amorphous alloys (Ref 6:231). In this study, the room temperature spectra of  $\text{Fe}_{80}\text{P}_{11.7}\text{C}_{6.3}\text{Si}_2$  differ significantly only in peak heights. As previously discussed, the peak height ratios generated by the model are of questionable value. Similar compositions could lead to similar values for the internal magnetic fields, and to different preferential directions of spin, or angular dependence of the Zeeman effect. The different values of isomer shift obtained indicate that the two spectra are unique, but further study is indicated to determine if these two materials do have unique spectra.

While the model has failed to describe adequately the materials, the consistent increase in the value of Chi-squared obtained with decreasing temperature, combined with the visual change in the spectra, indicates a change in the structure of the materials with decreasing temperature.

The wide range of values of Chi-squared also implies differences in the structures of the various materials, even at room temperature. A single model may not be sufficient to describe all of the materials.



### Summary

In summary, the solid solution twelve site model was inadequate to describe fully the materials analyzed. This conclusion is primarily based on the values of Chi-squared and linewidth obtained in the curve fits. Further research is indicated to determine which portions of the model need to be revised, and whether the two exceptions noted can be fully described by the model. The model has established significant trends in the various spectra, and may therefore be a valuable tool in establishing the initial values that would be required in using a more complex model of the amorphous structure of these materials. Finally, the results of this study indicate that the model used may be temperature dependent at lower temperatures, as Tsuei's results indicated at above room temperature (Ref 8).

### Recommendations

An evaluation of these materials using the iron-rich body centered cubic model of Fujita would be the next logical step in the analysis of these amorphous materials. A jump to the use of all 14 sites is, however, not recommended. A progression in the number of sites (and interstitial sites) considered should be made until acceptable values of linewidth are obtained. This recommendation is based on a conviction that the minimum number of sites considered with consistent results will be the most reasonable approximation to the true structure of the materials.

The second recommendation is that regardless of the



model assume in future studies, spectra should be obtained throughout the range of temperatures from liquid nitrogen to room temperature. It remains to be determined whether the changes with temperature noted in this study are gradual over the range, or represent phase changes occurring at a specific temperature.

The results obtained with seven percent boron and two percent silicon require confirmation. The remaining samples of parent plus silicon (not examined in this study) need to be evaluated to determine if they exhibit the same characteristics. In addition, confirmation that the changes noted are material, and not manufacture dependent, is required. Only one sample of each material was available in this study.

A final recommendation is that the results of this study be compared with the x-ray diffraction and other tests now being accomplished by the Air Force Materials Laboratory.

## Bibliography

1. Spaepen, F. and D. Turnbull. "A Mechanism for the Flow and Fracture of Metallic Glasses." Scripta Metallurgica, 8: 563-568 (1974).
2. Polk, D. E. and D. Turnbull. "Flow of Melt and Glass Forms of Metallic Alloys." Acta Metallurgica, 20: 493-498 (April 1972).
3. Turnbull, D. Studies on the Transformations, Thermal Behavior, and Structure of Amorphous Materials: Covalently Bound and Metallic. Office of Naval Research Report, NR 032-485. Harvard University, 1973.
4. May, Leopold. An Introduction to Mossbauer Spectroscopy. New York: Plenum Press, 1971.
5. Goldanskii, V. I. and R. H. Heber. Chemical Applications of Mossbauer Spectroscopy. New York: Academic Press, 1968.
6. Fujita, F. E. "Mossbauer Spectroscopy in Physical Metallurgy" in Topics in Applied Physics. Vol 5: Mossbauer Spectroscopy, edited by Uli Gonser. New York: Springer-Verlag, 1975.
7. Polk, D. E. "The Structure of Glassy Metallic Alloys." Acta Metallurgica, 20: 485-491 (April 1972).
8. Tsuei, C. C., et al. "Temperature Dependence of the Magnetization of an Amorphous Ferromagnet." Physical Review, 170: 603-606 (June 1968).
9. Wertheim, Gunther K. Mossbauer Effect: Principles and Applications. New York: Academic Press, 1964.
10. Skluzacek, Eugene W. Analysis of the Mossbauer Spectra of NdCO<sub>5</sub>. AFML-TR-75-162. Wright-Patterson Air Force Base, Ohio: Air Force Materials Laboratory, 1976.
11. Shimony, U. "Condition for Maximum Single-Line Mossbauer Absorption." Nuclear Instruments and Methods, 37: 348-350 (1965).
12. Gonser, Uli. "From a Strange Effect to Mossbauer Spectroscopy" in Topics in Applied Physics. Vol 5: Mossbauer Spectroscopy, edited by Uli Gonser. New York: Springer-Verlag, 1975.

## Appendix A

### Program GENFIT and Subroutine READIN

Program GENFIT is the controlling routine for the least squares fitting program used in this study. As obtained, the program was designed for either Mossbauer or general curve fitting use. To reduce execution time and simplify use, this portion of the program was significantly rewritten. Similarly, subroutine READIN was modified to be compatible with the revised main program, and was also modified to accept data in a new format.

The input for both of these routines is read from cards in the following order and consists of:

1. Two cards containing the spectrum title or desired comments. Each of these cards may contain up to 80 characters. The information is stored in array TITL.
2. One card with six integer values separated by commas or blank spaces. These variables, and the order in which they should appear, are:
  - a. NPAR: the number of variables to be used in subroutine CALFUN to describe the spectrum.
  - b. VMAX1: the maximum channel number of the left branch of the velocity spectra prior to zero area irregularities.
  - c. VMIN2: minimum channel number of velocity spectra in right branch after zero area irregularities.
  - d. TOVR: the number of overflows in the time base

oscillator counts.

- e. IPLOT: Control parameter for the type of output plot desired:

IPLOT=0 CALCOMP plot of experimental and calculated spectra

IPLOT=10 Line printer plot of experimental and calculated spectra

IPLOT=any other value CALCOMP plot of experimental data, calculated spectrum, F-contribution, and residuals

- f. MAXFUN: The maximum number of calls of subroutine CALFUN desired.

3. NPAR cards with the name of the variable in the first six columns, and the initial estimate of the value in columns six through twelve. These cards are read in an A6E6 format and may be combined onto one or two cards in consecutive fields of twelve columns.
4. Forty cards containing the raw data as generated by established tape processing program.
5. One card with a variable number of integer values, read in free field format, in the following order:
  - a. ORDER: The order of the polynomial velocity fit desired.
  - b. DOVR: The number of overflows in the Mossbauer data. If the data has not completely overflowed, the higher value is used.



c. NZONES: The number of zones to be used in the background polynomial fit.

d. ZONEL and ZONER: The start and stop channel numbers of the number of zones specified in c.

A listing of the revised GENFIT main program and the READIN subroutine are included in this appendix.

```

PROGRAM GENFIT(INPUT,OUTPUT,TAPES=INPUT,PLOT)
C THE PROGRAM GENFIT WAS DEVELOPED BY BRUCE J. 7ABRANSKY
C OF THE ANL. THIS VERSION DELETES THOSE SECTIONS NOT
C REQUIRED FOR AFIT MOSSBAUER STUDIES. MODIFICATIONS WERE
C MADE BY TERRY A. SCHMIDT.
C
C ***** 28 FEB 78 *****
COMMON W(10000),XD(402),YD(402),YC(402),YDY(402),FS1(402)
COMMON YCX(100)
COMMON /FREQAP/TOVR,MPLX,BACKGRD
COMMON /NAM/ XINIT(20),FRM(20),ERX(20)
COMMON /HEADING / TITL(18)
COMMON /CALF/ IFLAG
COMMON /PLOTS/ IPLOT
DIMENSION F(402),X(20),F(20)
DIMENSION F(402),X(20),F(20)
INTEGER BACKGRD,TOVR,VMAX1,VMIN2

C READ IN THE FIRST TITLE CARD.
10 READ 330,(TITL(I),I=1,8)
C
C IF THE FIRST TITLE CARD IS AN END OF FILE CARD, END PROGRAM.
IF(EOF(5))73,25
C
C READ IN THE SECOND TITLE CARD AND ONE CARD FOR CONTROL PARAMETERS.
C THESE VARIABLES ARE:
C
C NPAR: THE NUMBER OF PARAMETERS USED TO DESCRIBE THE SPECTRUM
C
C VMAX1: MAXIMUM CHANNEL NUMBER OF VELOCITY DATA IN LEFT
C        BRANCH BEFORE ZERO AREA IRREGULARITIES
C
C VMIN2: MINIMUM CHANNEL NUMBER OF VELOCITY DATA IN RIGHT
C        BRANCH AFTER ZERO AREA IRREGULARITIES
C
000100
000110
000120
000130
000140
000150
000160
000170
000180
000190
000200
000210
000220
000230
000240
000250
000260
000270
000280
000290
000300
000310
000320
000330
000340
000350
000360
000370
000380
000390
000400
000410
000420
000430
000440
000450

```

```

C      TOVR: THE NUMBER OF OVEFFLOWS IN THE TIME BASE OSCILLATOR
C      IPLOT: IPLOT CONTROLS THE TYPE OF PLOT GENERATED BY GENFIT.
C      VALUES OF IPLOT AND THE CORRESPONDING TYPES OF PLOT ARE:
C      0: ONLY THE DATA AND CALCULATED SPECTRUM ARE PLOTTED
C      (CALCOMP)
C      1: DATA, CALCULATED SPECTRUM, F-CONTRIBUTION AND
C      RESIDUALS ARE PLOTTED. (CALCOMP)
C      10: DATA AND CALCULATED SPECTRUM ARE PLOTTED ON THE
C      LINE PRINTER
C      MAXFUN: THE MAXIMUM NUMBER OF CALLS OF CALFUN DESIRED
C      READ 390, (ITIL(I), I=9, 16)
C      READ *, NPAR, VMAX1, VMIN2, TOVR, IPLOT, MAXFUN
C      C SET CONTROL PARAMETERS
C      FSIZE=100.0
C      IPRINT=0
C      FSCALE=100.0
C      IFIT=0
C      IDUN=0
C      MLEX=10
C      BACKGRD=2
C      ILAG=1
C      C READ IN LABELS OF PARAMETERS AND INITIAL GUESSES FOR PARAMETERS
C      THESE ARE READ IN A A6,EE FORMAT
C      DO 20 I=1, NPAR
C      READ 410, PRM(I), X(I)
C      DO 30 I=1, NPAR

```

000460  
000470  
000480  
000490  
000500  
000510  
000520  
000530  
000540  
000550  
000560  
000570  
000580  
000590  
000600  
000610  
000620  
000630  
000640  
000650  
000660  
000670  
000680  
000690  
000700  
000710  
000720  
000730  
000740  
000750  
000760  
000770  
000780  
000790  
000800  
000810

```

30      XINIT(I)=X(I)
C
C CALL THE READIN SUBROUTINE . IT WILL READ IN THE DATA AND STORE
C THE X AND Y VALUES OF THE DATA POINTS TO BE USED IN THE MINIMIZATION
C IN THE UNLABELED COMMON BLOCK AS XD AND YD, UP TO 400 OF EACH.
      CALL READIN(IFIT,IRUN,VMAX1,VMIN2,TOVR,MPLX,BACKGRD,NP)
C
C CALCULATE THE F'S, USED TO INDICATE WHEN CONVERGENCE IS REACHED
      E(1)=SQRT (X(1))/ESIZE
      DO 40 I=2,NPAR
        E(I)=X(I)/ESIZE
40
C
C VA02A STARTS THE MINIMIZATION AND CALLS CALFUN
      CALL VA02A (NP,NPAR,F,X,E,ESCALE,IPRINT,MAXFUN)
C
C PRINTING FROM CALFUN IS NOW ACCOMPLISHED
      IFLAG=0
      CHI2=0
      CALL CALFUN (NP,NPAR,F,X)
C
C YDY AND YCY ARE THE POINTS PLOTTED IN GOPLOT. FOR MOSSBAUER
C RUNS THEY ARE DEFINED BELOW.
      PRINT 440
      DO 50 I=1,NP
        YDY(I)=1.-YD(I)/X(1)
        YCY(I)=1.-YC(I)/X(1)
        FSQ(I)=F(I)**2
        CHI2=CHI2+FSQ(I)
50
C
C PRINTED OUTPUT FOR MOSSBAUER RUNS
      PRINT 450, XD(I),YD(I),YC(I),F(I),FSQ(I),YDY(I),YCY(I)
C
C SUBROUTINE SV01A COMPUTES THE ERROR MATRIX:
C THE SQUARE ROOT OF THE DIAGONALS OF THE ERROR MATRIX IS
C CALCULATED AND USED AS THE ERRORS ON THE PARAMETERS
      CALL SV01A (NP,NPAR,ERMAT,20,2)

```

000820  
000830  
000840  
000850  
000860  
000870  
000880  
000890  
000900  
000910  
000920  
000930  
000940  
000950  
000960  
000970  
000980  
000990  
001000  
001010  
001020  
001030  
001040  
001050  
001060  
001070  
001080  
001090  
001100  
001110  
001120  
001130  
001140  
001150  
001160  
001170



[illegible]

[illegible]

```

C      NZONES : NUMBER OF ZONES TO BE USED FOR THE BACKGROUND
C      POLYNOMIAL FIT
C
C      ZONEL AND ZONER : START AND STOP CHANNELS FOR EACH OF THE
C      NUMBER OF ZONES SELECTED
C
C      THESE PARAMETERS MUST BE INTEGER VALUES AND ARE READ IN FREE
C      FIELD FORMAT
C
C      READ*, ORDER, DOVR, NZONES, (ZONEL(I), ZONER(I), I=1, NZONES)
C      PRINT 909, (ITIL(I), I=1, 8)
C      PRINT 909, (ITIL(I), I=9, 16)
C      PRINT 903, VMAX1, VMIN2, TOVR, MPLEX, ORDER, DOVR,
C      2 (ZONEL(I), ZONER(I), I=1, NZONES)
C
C      CONVERT FROM CHANNEL NUMBERS TO ARRAY LOCATIONS
C
C      J1=ZONEL(1)+1
C      J2=ZONER(NZONES)+1
C      VMAX1=VMAX1+1
C      VMIN2=VMIN2+1
C
C      FIND AND CORRECT FOR OVERFLOWS IN VELOCITY DATA
C
C      I=0
C      DO 1 I=29, VMAX1, MPLEX
C      JUMP=DATA(I+MPLEX)-DATA(I)
C      IF (JUMP.GE.500000) III=III+1
C      CONTINUE
C      DO 2 I=29, VMAX1, MPLEX
C      JUMP=DATA(I+MPLEX)-DATA(I)
C      DATA(I)=DATA(I)+III*1000000
C      IF (JUMP.GE.500000) III=III+1
C      CONTINUE

```

001910  
001920  
001930  
001940  
001950  
001960  
001970  
001980  
001990  
002000  
002010  
002020  
002030  
002040  
002050  
002060  
002070  
002080  
002090  
002100  
002110  
002120  
002130  
002140  
002150  
002160  
002170  
002180  
002190  
002200  
002210  
002220  
002230  
002240  
002250  
002260



```

002270 IF(III.NE.0) PRINT 906
002280 LL=399-MPLEX
002290 DO 3 I=VMIN2,LL,MPLX
002300 JI4P=DATA(I)-DATA(I+MPLFX)
002310 DATA(I)=DATA(I)+III*1000000
002320 IF(JUMP.GE.500000) III=III+1
002330 CONTINUE
002340
002350
002360
002370
002380
002390
002400
002410
002420
002430
002440
002450
002460
002470
002480
002490
002500
002510
002520
002530
002540
002550
002560
002570
002580
002590
002600
002610
002620

3
C PRINT INPUT DATA WITH VELOCITY DATA CORRECTED FOR OVERFLOWS
C
C
    PRINT901
    PRINT*, " "
    PRINT*, " CHANNEL    COUNTS:"
    J=J
    DO 4 I=1,40
    K=10*I-3
    L=K+9
    PRINT 908,J,(DATA(M),M=K,L)
    J=J+10
    CONTINUE
4
C
C FIND AVERAGE NUMBER OF OSCILLATOR COUNTS
C
    TIME=0.
    DO 10 I=4,15
    TIME=TIME+DATA(I)+(10**6)*TOVR
    TIME=TIME/13.
10
C
C CONVERT VELOCITY DATA TO VELOCITIES AND FIND POLYNOMIAL
C
C FFT TO DESIRED ORDER
C
    J=0
    DO 15 I=29,VMAX1,MPLX
    J=J+1
    X(J)=FLOAT(I)
    Y(J)=DATA(I)*156.25/TIME*(-1.)
15

```



```

00 16 I=VMIN2,389,MPLX
J=J+1
X(J)=FLOAT(I)
Y(J)=DATA(I)*156.25/TIME
CALL PLSQ(X,Y,J,ORDER,VCP,1,EMAX,ERMS,EMEQ)
16
C
C CORRECT DATA FOR NUMBER OF OVERFLOWS AND FIND
C THE BACKGROUND POLYNOMIAL FIT
C
DUMMY=DATA(J1)
00 25 I=1,400
IF(DOVR.LT.0) GO TO 899
IF(MOD(I+1,MPLX).EQ.0) GO TO 25
IF(I.LT.J1)GO TO 25
IF(DUMMY-DATA(I).GT.500000) DOVR=DOVR+1
IF(DATA(I)-DUMMY.GT.500000) DOVR=DOVR-1
DUMMY=DATA(I)
DATA(I)=DATA(I)+(10**6)*DOVR
25 X(I)=FLOAT(I)
K=0
00 30 I=1,NZONES
J1=ZONEL(I)+1
J2=ZONER(I)+1
00 29 J=J1,J2
IF(MOD(J+1,MPLX).EQ.0)GO TO 29
K=K+1
X(K)=FLOAT(J)
Y(K)=DATA(J)
29 CONTINUE
30 CONTINUE
CALL PLSQ(XF,YF,K,BACKGRD,C,0,EMAX,ERMS,EMEQ)
C
C LOAD CALCULATED VELOCITY AND MOSSBAUER DATA INTO COMMON FOR
C GENFIT MAIN PROGRAM
C
C NOTE: THIS SECTION CORRECTS FOR BACKGROUND FIT
C
002630
002640
002650
002660
002670
002680
002690
002700
002710
002720
002730
002740
002750
002760
002770
002780
002790
002800
002810
002820
002830
002840
002850
002860
002870
002880
002890
002900
002910
002920
002930
002940
002950
002960
002970
002980

```

THIS PAGE IS BEST QUALITY PRACTICABLE  
FROM COPY FURNISHED TO DDC

002990  
003000  
003010  
003020  
003030  
003040  
003050  
003060  
003070  
003080  
003090  
003100  
003110  
003120  
003130  
003140  
003150  
003160  
003170  
003180  
003190  
003200  
003210  
003220  
003230  
003240  
003250  
003260  
003270  
003280  
003290  
003300  
003310

```

J1=ZONEL(1)+1
L=ORDER+1
K=0
DO 35 I=J1,385
  IF(MOD(I+1,MPLX).EQ.0) GO TO 35
  K=K+1
  Y(K)=DATA(I)-(C(1)*I**2+C(2)*I+C(3))+XINIT(1)
  X(K)=0.
  DO 44 J=1,L
    X(K)=XD(K)+VCP(J)*I**(L-J)
  CONTINUE
  N=K
  RETURN
  PRINT 906
  PRINT 904
  PRINT 905,(I,XD(I),YD(I),I=1,NP)
  FORMAT(3X,10I7)
  FORMAT(23H DATA BLOCK AS READ IN,/)
  2,I3,* AND FROM *,I3,* TO 398*/* THERE ARE*,I3,
  3* OVERFLOWS IN THE TIME BASE AND THE MPX OPTION IS*,
  4I3, /* THE VELOCITY FIT WILL BE OF ORDER*,I3/
  5* THERE ARE*,I3,* MILLION COUNTS TO BE ADDED TO THE YOSSBAUER
  6DATA*/* THE PARABOLA BASELINE WILL BE FITTED TO CHANNELS: *
  7,I3,* TO*,I3,9(*; *,I3,* TO *,I3))
  FORMAT(1H1,+(34 INDEX,10H VELOCITY ,12H COUNTS ))
  904
  905 FORMAT(4(3X,I3,2X,F8.3,2X,E12.6))
  906 FORMAT(* THERE IS A CONTROL PARAMETER ERROR IN READIN.*)
  907 FORMAT(5E16.8)
  908 FORMAT(2X,I4,5X,10I9)
  909 FORMAT(1H1/1H 8A10/1H 8A10)
  RETURN
END

```

## Appendix B

### Subroutine CALFUN

Subroutine CALFUN is used to describe the calculated spectrum using 17 variables, adjusted by the GENFIT least-squares minimization routine. This version of CALFUN uses the simplified Hamiltonian, further reduced to a numerical form for speed of execution. In order to calculate the peak positions, the routine used variables of magnetic field (one for each assumed site), and isomer shift. To compute the Lorentzian line shapes, the routine uses the binomial probabilities multiplied by an artificial variable, called total intensity, to find individual site and peak intensities. To implement the model, linewidths are variable, with the restriction that the  $n$ th peak of each site will have the same linewidth. The factors called ratio  $[RAT(x)]$  allow the individual peak heights for a given site to assume whatever ratio yields the best fit--again with the restriction that the  $n$ th peak of each site be in the same ratio. Peak heights are normalized to peak six (the peak with the greatest positive velocity).

The final spectrum is the sum of the six sites' contributions, each consisting of six Lorentzian profiles centered at the velocities determined by the Hamiltonian.

A listing of the subroutine CALFUN is included in this appendix.

```

SUBROUTINE CALFUN(NP,NPAR,F,X)
C FPC CALFUN BASED ON ARTICLES BY GONSER AND TSUEI. THIS CALFUN FORCES
C A BINOMIAL DISTRIBUTION OF THE CONTRIBUTIONS FROM EACH SITE. TWELVE
C SITES ARE ASSUMED, HOWEVER ONLY THE CONTRIBUTIONS FROM THE SIX
C "STROGEST" SITES ARE CALCULATED. SEVENTEEN VARIABLES ARE USED,
C ALLOWING VARIATION OF H-FIELD, LINE WIDTH, PEAK RATIOS, AND ISOMER
C SHIFT. PEAK RATIOS ARE NORMALIZED TO PEAK 6: THE PEAK WITH THE
C GREATEST POSITIVE VELOCITY.
C
C RINOM MODIFIED 6 DEC 77
C
C THE REQUIRED VARIABLES ARE:
C
C BASE LINE
C
C SIX VALUES FOR H-FIELD
C
C TOTAL INTENSITY: AN ARTIFICIAL VALUE MULTIPLIED BY BINOMIAL
C PROBABILITIES TO OBTAIN SITE CONTRIBUTIONS
C
C THREE VALUES FOR LINE WIDTHS: REPRESENTING THE LINE WIDTHS FOR
C THREE SYMMETRICAL SETS OF PEAKS
C
C ISOMER SHIFT
C
C FIVE VALUES FOR THE RATIOS OF PEAKS ONE THRU FIVE TO PEAK SIX
COMMON W(10000),XD(402),YD(402),YC(402),YDY(402),YCY(402),FSQ(402)
COMMON /HEADING/TITL(18)
COMMON /NAM/XINIT(20),PFM(20),ERX(20)
COMMON /CALF/ IFLAG

```



```

009700 DIMENSION F(402),X(20)
009710 REAL V(5,6),P(5)
009720
009730 C LOAD VALUES OF BINOMIAL PROBABILITIES
009740 C
009750 DATA (P(I),I=1,6)/.0687,.2062,.2835,.2362,.1329,.0532/
009760 C
009770 C LOAD VALUES OF CONSTANTS FOR HAMILTONIAN
009780 C
009790 DATA A,D,C/.016087024,.0093151213,.002543187/
009800 C
009810 IF(IFLAG)25,25,10
009820 C
009830 C IF IFLAG IS NOT POSITIVE CALFUN IS BEING CALLED FOR PRINTING ONLY
009840 C
009850 10 CONTINUE
009860 C
009870 C CALCULATE PEAK VELOCITIES FOR EACH SITE
009880 C
009890 DO 20 J=1,6
009900 V(J,1)=-A*X(J+1)+X(12)
009910 V(J,2)=-D*X(J+1)+X(12)
009920 V(J,3)=-C*X(J+1)+X(12)
009930 V(J,4)=C*X(J+1)+X(12)
009940 V(J,5)=D*X(J+1)+X(12)
009950 V(J,6)=A*X(J+1)+X(12)
009960 CONTINUE
009970 C
009980 C CALCULATE THE SPECTRUM
009990 C
010000 DO 30 I=1,NP
010010 YC(I)=0.0
010020 DO 35 J=1,6

```

```

010030
010040
010050
010060
010070
010080
010090
010100
010110
010120
010130
010140
010150
010160
010170
010180
010190
010200
010210
010220
010230
010240
010250
010260
010270
010280
010290
010300
010310

01 35 K=1,6
IF(K.EQ.5) GO TO 36
TI=ABS(X(8))*P(J)*X(K+12)
GO TO 37
TI=ABS(X(6))*P(J)
CONTINUE
R=X(11)
IF(K.EQ.1.OR.K.EQ.6) R=X(9)
IF(K.EQ.2.OR.K.EQ.5) R=X(10)
YC(I)=YC(I)+TI/(((XD(I)-V(J,K))**2*4)/R**2)+1)
YC(I)=(1.0-YC(I))*X(1)
F(I)=(YD(I)-YC(I))/SORT(YD(I))
RETURN

C ON THE FINAL CALL OF CALFUN PRINT THE PEAK VELOCITIES FOR EACH SITE
C
25 CONTINUE
PRINT*, " "
PRINT*, " "
PRINT*, " THE PEAK VELOCITIES FOR EACH SITE ARE:"
PRINT*, " "
GO 26 I=1,6
PRINT*, " "
PRINT*, " FOR SITE NUMBER ", I
PRINT 100, (V(I,L), L=1,6)
CONTINUE
26 FORMAT(5X,6F10.4)
100 RETURN
END

```

### Vita

Terry Allen Schmidt was born on March 17, 1943, in Milwaukee, Wisconsin, and is the son of Howard W. Schmidt and Beverley M. Schmidt. He graduated from Solomon Juneau High School in Milwaukee, Wisconsin, in January of 1961. In June of 1962, he graduated from the United States Air Force Academy Preparatory School, and, in 1966, from the United States Air Force Academy with a degree of Bachelor of Science in military sciences. After graduation from the Air Force Academy, he completed pilot training and conversion into the C-130 aircraft. Prior to attending the Air Force Institute of Technology, he served as an aircraft commander and instructor pilot at Ching Chaun Kaung AB, Republic of China; Dyess AFB, Texas; RAAF Base Richmond, Richmond, New South Wales, Australia; and Little Rock AFB, Arkansas. He and his wife Denise have no children.

Permanent address: 3605 Neely

Midland, Texas 79701

UNCLASSIFIED

SECURITY CLASSIFICATION OF THIS PAGE (When Data Entered)

REPORT DOCUMENTATION PAGE		READ INSTRUCTIONS BEFORE COMPLETING FORM
1. REPORT NUMBER GNE/PH/78M-8	2. GOVT ACCESSION NO.	3. RECIPIENT'S CATALOG NUMBER
4. TITLE (and Subtitle) AN ANALYSIS OF METALLIC GLASSES BY MOSSBAUER SPECTROSCOPY.		5. TYPE OF REPORT & PERIOD COVERED MS Thesis Masters thesis
7. AUTHOR(s) Terry A. Schmidt		6. PERFORMING ORG. REPORT NUMBER
9. PERFORMING ORGANIZATION NAME AND ADDRESS Air Force Institute of Technology (AFIT-EN) Wright-Patterson AFB, Ohio 45433		8. CONTRACT OR GRANT NUMBER(s)
11. CONTROLLING OFFICE NAME AND ADDRESS		10. PROGRAM ELEMENT, PROJECT, TASK AREA & WORK UNIT NUMBERS
14. MONITORING AGENCY NAME & ADDRESS (if different from Controlling Office)		12. REPORT DATE March 1978
		13. NUMBER OF PAGES 1275 P.
		15. SECURITY CLASS. (of this report) Unclassified
		15a. DECLASSIFICATION/DOWNGRADING SCHEDULE
16. DISTRIBUTION STATEMENT (of this Report)  Approved for public release; distribution unlimited		
17. DISTRIBUTION STATEMENT (of the abstract entered in Block 20, if different from Report)		
18. SUPPLEMENTARY NOTES Approved for public release; IAW AFR 190-17 JERRAL F. GUESS, Captain, USAF Director of Information		
19. KEY WORDS (Continue on reverse side if necessary and identify by block number) Metallic Glasses Amorphous Mossbauer		
20. ABSTRACT (Continue on reverse side if necessary and identify by block number) Several models have been used to describe the structure of iron-phosphorous-carbon amorphous alloys. In this study a twelve site substitutional solid model is used to describe the Mossbauer spectra obtained from six different metallic amorphous alloys. Spectra were obtained at room and at liquid nitrogen temperatures for the parent material, as well as for alloys containing various percentages of boron or silicon. Each spectrum is fit with a sum of Lorentzian profiles describing the twelve site model. The		

DD FORM 1473

1 JAN 73

EDITION OF 1 NOV 65 IS OBSOLETE

UNCLASSIFIED

SECURITY CLASSIFICATION OF THIS PAGE (When Data Entered)

012200


3rd page  
ke



UNCLASSIFIED

SECURITY CLASSIFICATION OF THIS PAGE(When Data Entered)

results indicate that the model is inadequate in fully describing the structure of the various materials. The results also indicate a difference in structure between the materials, and, in two cases, significant changes in structure with decreased temperature.



UNCLASSIFIED

SECURITY CLASSIFICATION OF THIS PAGE(When Data Entered)